Chapter 2
Earth Observation Systems

2.1 Introduction

With an introduction to remote sensing in Chap. 1, we will now move on to the sensors and the major Earth-observing systems providing the spectral measurements that enable us deriving information on natural resources and environment. As discussed in Chap. 1, a remote sensing system consists mainly of instrumentation/sensor, processing and analysis/interpretation designed to measure, monitor, and predict the physical, chemical, and biological aspects of the Earth's system. This chapter addresses remote sensors/instruments and platforms. Before proceeding to the Earth-observing systems it would be appropriate to familiarize ourselves with the remote sensing platforms, and the kind of sensors used for capturing images of the Earth and environment.

2.2 Sensing Platforms

The remote sensing platform refers to any system onto which remote sensing sensors are mounted. Tripod stand, cherry-pickers, towers, crane, tall buildings or scaffolding, balloons, aircrafts, rockets and satellites are examples of remote sensing platforms as in Fig. 2.1. The purpose of platform is to position the sensor over an area of interest. The type of platform therefore is determined by the requirements of the measurements to be made. For small-scale infrequent monitoring, or calibration purposes simple handheld instruments or instruments mounted on fixed platforms (tower, masts, etc.) may be sufficient.

R. S. Dwivedi, *Remote Sensing of Soils*,
DOI 10.1007/978-3-662-53740-4_2

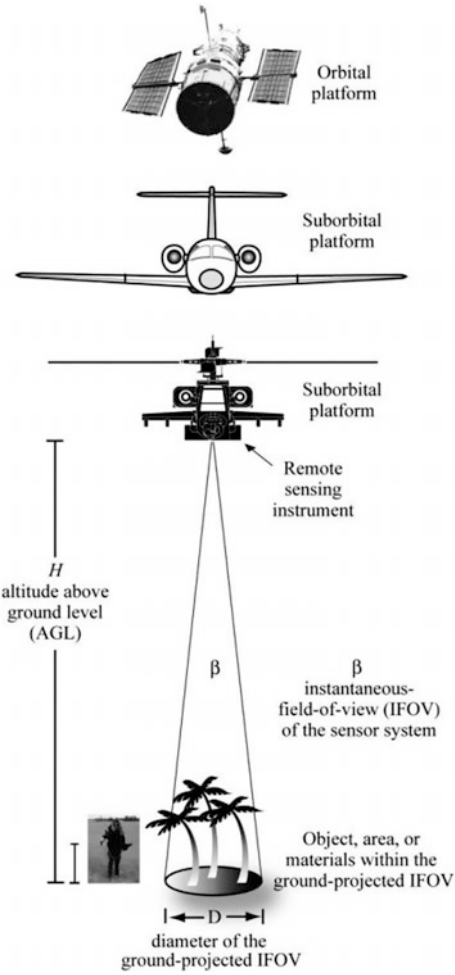

Fig. 2.1 Remote sensing platforms

2.2.1 Airborne Platforms

A great deal of remote sensing studies have been conducted, and still being done, using aircrafts of various types as a platform. However, balloons are also sometimes used for studies related to atmospheric applications. Besides, unmanned aerial vehicles (UAVs) are being increasingly used for various applications involving smaller aerial extent. The major advantage of aircrafts is their versatility. Aircrafts can be flown at short notice where and when required, of course subject to weather conditions. The flying height can be altered to adjust the scale of the photo or image or to fly under cloud cover. Besides, their flight lines can be arranged for specific purposes so as to cover a specific area, to observe that area from a particular angle or to produce overlapping images for stereoscopy. Disadvantages include higher

cost of flying operation, seeking permission from competent authorities in some countries, and instability of the aerial platforms and images may suffer from various distortions due to drift, yaw, roll and pitch, and positioning of the aircraft may be slightly uncertain, and is not reproducible.

2.2.2 Spaceborne Platforms

The use of satellites as a platform began in 1960. In fact, it was on 1 April 1960 when the first low-Earth orbit Television Infrared Observation Satellite (TIROS-1) Earth-observing mission was launched. This stepping stone has provided stimulus to the design, development and launch of several Earth observation satellites. Satellites are placed in orbits that are designed for the specific purposes of the mission, and to suit the particular characteristics of the instrument(s) on-board. There are two main classes of orbits, namely *geostationary* orbit and the *low-Earth* or *near-polar* orbit.

2.2.2.1 Near-Polar Orbits

Most Earth observation satellites are in near-polar orbits that range from 600 to 2000 km above the ground. With the Earth's radius of about 6300 km, such satellites take about 100 min to complete one orbit. If such an orbit passes over the Earth's poles, the subsatellite track would always pass through the same points on the Earth's surface. As a result, only that particular track would be observed by the sensor on-board. If, however, orbits are slightly inclined away from the poles, then the orbit would *precess* with respect to the Earth and subsequent tracks (paths) would be displaced by an amount that depends on the angle made by the plane of the satellite orbit and the Earth's rotational axis. The rate of precession will determine the number of orbits required before the satellite track repeats itself, and the time taken to accomplish it will be the satellite revisit time, i.e. the time between successive observations of a particular point on the Earth's surface. Such orbits are called *polar orbits* or more correctly *near-polar orbits.* A special case of a polar orbit is one where the orbital precession is exactly equal to the Earth's solar precession, so that the satellite crosses the equator at exactly the same local solar time each orbit. Such an orbit is referred to as *Sun-synchronous orbit* (Fig. 2.2a, b). The advantage of this type of orbit is that the solar angle is approximately the same each time a point is imaged, and hence variability of illumination and shadow angles will be minimized. This makes them particularly suitable for monitoring highly dynamic features like vegetation.

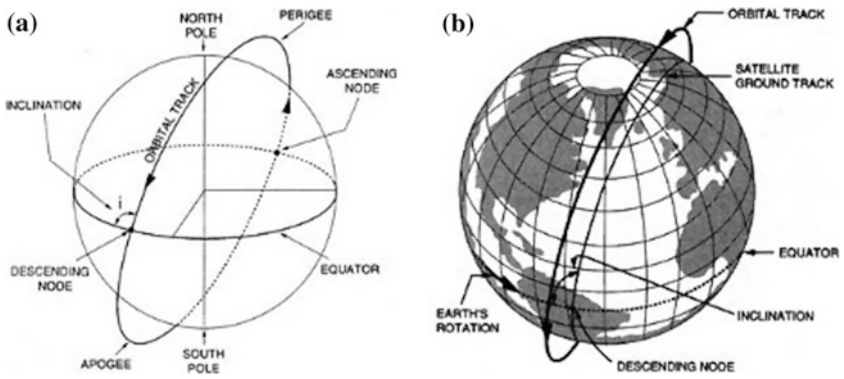

Fig. 2.2 **a** The definition of satellite orbits. **b** Schematic representation of a Sun-synchronous orbit

2.2.2.2 Geosynchronous Orbits

A geosynchronous orbit is an orbit around the Earth with an orbital period of one sidereal day, intentionally matching the Earth's sidereal rotation period. In fact, at a height of about 35,786 km, the orbital period of a satellite is approximately 23 h 56 min and 4 s. If a satellite is placed in an orbit exactly over the equator at this height, and is travelling in the same direction as the Earth is rotating (e.g. west to east), then as the satellite progresses, the Earth revolves around its axis underneath it with exactly same rotational velocity. As a result, the satellite appears to remain in position over a point on the equator. Such an orbit sometimes is referred to as *Clarke orbit.* Such an orbit is *preferred* for communication satellites as they remain in view of small fixed antennae and give continuous reception. There are several meteorological satellites, namely Meteosat, GOES, GOMS, INSAT, etc. distributed around the equator, each viewing nearly 40% of the Earth's surface and providing almost continuous coverage of the global weather patterns. Figure 2.3 shows the schematic representation of a geostationary orbit.

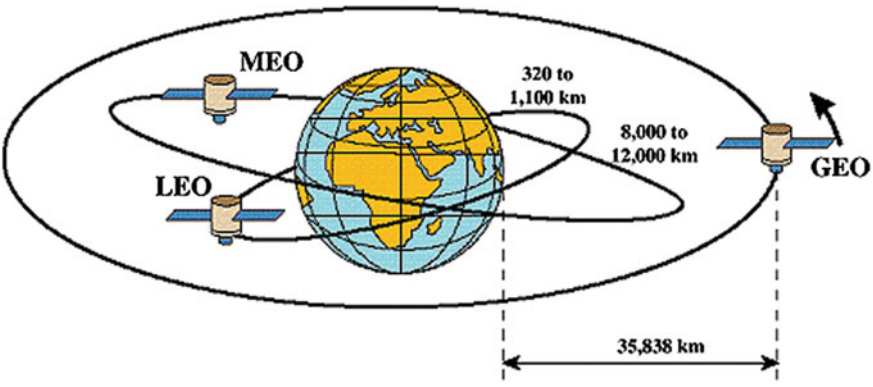

Fig. 2.3 Schematic representation of a geostationary orbit

2.3 Sensors

Remote sensing sensors are instruments that measure the properties of electromagnetic radiation leaving a surface/medium due to reflection, scattering or emission. Sensors have been developed to utilize specific properties of electromagnetic radiation such as wavelength, polarization, interaction with different surfaces and speed of propagation in order to enable the interpreter/analyst to extract such quantities from the data produced. Generally, radiance is the property measured and it is measured as a function of wavelength, but could include other parameters such as the state of polarization as well. This information could be collected over a spatial extent including the angular dependence of the observation and in certain cases, such as atmospheric sounding, as a function of distance along the line of sight of the instrument. Imagers, radiometers, spectrometers, profilers or rangers like radar and LiDAR are examples of remote sensing sensors. Sensors have also been categorized based on the region of the electromagnetic spectrum they are sensitive to (e.g. optical lens, microwave sensors) and source of illuminating the target/feature (e.g. active and passive sensors). As mentioned in Sect. 1.1 of Chap. 1 radar and LiDAR are *active* sensors since they provide their own pulse of energy. Most other sensors are *passive* because they use electromagnetic energy provided by the Sun or the Earth. A brief description of the passive and active sensors is given hereunder.

2.3.1 Optical Sensors

The optical sensors are those sensors whose response covers a wavelength region extending from about 0.4 to 20 μm which is considered an optical-IR (OIR) sensor. Since the radiation reception and analysis are carried out by instruments which are built on optical technology—lenses, mirrors, prisms, grating, etc, the optical sensors can be further grouped into two main categories—photographic and electro-optical sensors. In case of electro-optical sensors, the optical image is first converted into an electrical signal (video data) and further processed to record or transmit the data.

2.3.1.1 Photographic Cameras

Photographic cameras consist of a lens assembly and the film magazine. The lens cone assembly includes the lens, filter, shutter and diaphragm (Fig. 2.4). The lens is usually a multi-element lens assembly. The filter limits the wavelength region of the scene radiance reaching the film. Filters are transparent (glass or gelatin) materials placed in front of the lens, the most common being the absorption films, which absorb certain wavelengths. The diaphragm (aperture stop) is located in between the lens elements. The diaphragm controls the aperture of the lens which decides the amount of light passing through the lens. The diaphragm diameter can be adjusted to

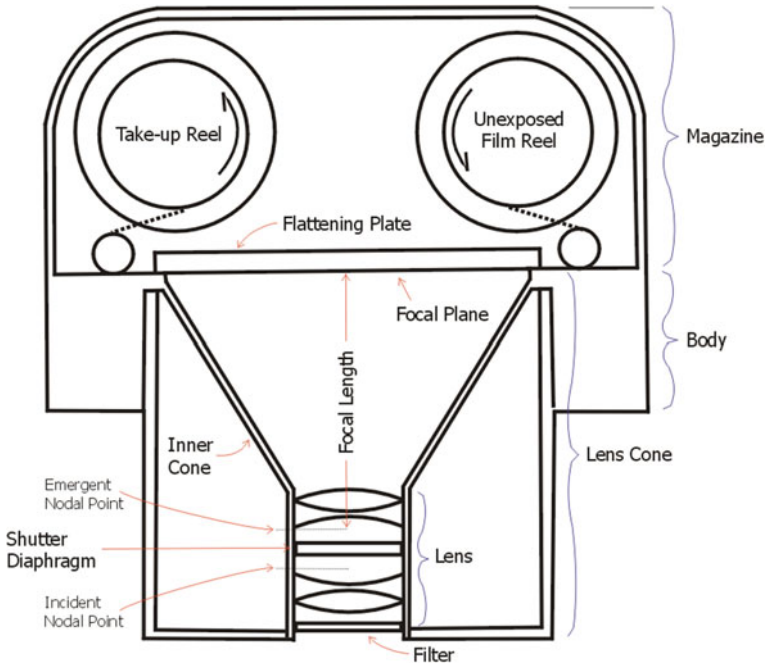

Fig. 2.4 Sketch of a typical mapping camera

suit lighting conditions and film sensitivity. The shutter controls the duration of the exposure. The shutter is incorporated at the focal plane or within the lens assembly.

The camera magazine, which holds the film supply and take up reels, can be invariably detached from the camera. During exposure, the film is held stationary and flat at the focal plane. For cameras designed for precision measurement, a vacuum system usually ensures this. A camera body to which the lens cone and the film magazine are attached also contains the film drive mechanism. The most commonly used camera is the mapping camera—generally referred to as metric camera or cartographic camera (Fig. 2.5). The important feature of the mapping camera is its high degree of distortion correction and provision for fixed marks (fiducial marks) to be recorded on the film. The lens has a fixed focal length and is rigidly fixed relative to the film plane. The fiducial markers are exposed on film simultaneously with the exposure of ground scene. The camera can be operated with varying overlaps to produce stereoscopic pairs to generate height information.

The scale of aerial photographs can be determined as follows (Fig. 2.6):

$$\text{scale} = \frac{\text{f}}{\text{H}} = \frac{\text{f}}{\text{H} - \text{H}'}, \tag{2.1}$$

where f is the focal length of camera and H is the altitude above the ground (H−H′ from Fig. 2.6).

Fig. 2.5 One of the smaller models of aerial camera dated 1907 kept in Duetsches museum, Germany (Adapted from Curran 1988) (https://www.scribd.com/document/102236883/Aerial-Photography) Accessed on 24 July 2016

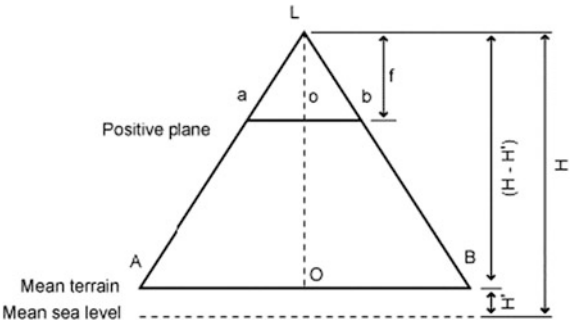

Fig. 2.6 Aerial photograph's scale

2.3.1.2 Digital Aerial Cameras

Digital aerial cameras are the advanced version of photographic cameras wherein the Charge Coupled Device (CCD) arrays are used in place of films to produce the image of the terrain features. Digital photography is capable of delivering photogrammetric accuracy and coverage as well as multispectral data at any user-defined resolution down to 0.1 m ground sampling distance. Digital aerial cameras typically have CCD arrays that produce images containing about 3000 × 2000 to 7000 × 5000 lines/pixels. Most record an 8-bit to 12-bit black-and-white image

(256-4096 grey levels). The shutter can be mechanical or electronic. The exposure time and aperture setting are adjusted before the overflight, depending on conditions and brightness of the mapped features. Each frame is instantaneously recorded so, unlike multispectral line scanners, there is a minimum distortion due to aircraft motion during acquisition. The aircraft altitude and the focal length of the lens system determine the ground resolution or ground sampling distance (GSD). Typical GSD values arrange from 15 cm to 3 m.

2.3.1.3 Video Cameras

In the video/vidicon/television camera, an optical system is made to focus the ground scene onto a photoconductive surface. The incident photons vary the conductivity of the surface locally according to the intensity of light. An electron beam is made to scan the photoconductive surface from the rear side. The resulting target current will be proportional to the conductivity of the photoconductive surface, hence the intensity of light. The signal is further amplified and recorded or transmitted. In the case of Return Beam Vidicon (RBV), the signal is derived from the depleted electron beam which is reflected from the photo-conducting surface. This is further amplified by a multi-stage electron multiplier. The Return Beam Vidicon (RBV) was used in the Landsat series (Eastman 1970) and the television camera system in the Indian experimental remote sensing satellites, Bhaskara-I and -II (Joseph 2003).

2.3.1.4 Radiometers

A radiometer is the basic element of all electro-optical and microwave sensors. In its simplest form, it is a device for measuring the intensity of electromagnetic radiation impinging on its detector within a defined spectral range. The technical detail depends upon the particular part of the electromagnetic spectrum the sensor is intended to operate. However, all radiometers comprise three elements (Rees 1999): an optical system to focus the radiation and to select the wavelength, detectors that produce an electrical signal, and a signal processor to provide an output. The simplest radiometers are non-imaging detectors that integrate the radiation that arrives from within a field of view and within a specific wave band. Handheld platform-mounted spectroradiometers with high spectral resolutions are often used in the field to measure the reflectance spectrum of particular targets or vegetation species, often as part of calibration process whereas radiometers mounted on aircrafts satellites measure the radiation from individual large areas of ground along the flight line or subsatellite track.

2.3.1.5 Electro-Optical Scanners

The opto-mechanical scanners operate in the visible (400–700 nm), the reflected infrared (700–3000 nm) and the thermal infrared (3000–14000 nm) region of the electromagnetic spectrum. After being focused by a mirror system, the radiation from each image element or pixel is segregated into spectral bands, with one image being produced in each spectral band. Depending on the mode of scanning electro-optical scanner could be grouped into the cross-track or whiskbroom and the along-track or push broom types. Push broom scanners, also sometimes referred to as along-track scanners, use a line of detectors arranged perpendicular to the flight direction of the spacecraft (Fig. 2.7). As the spacecraft moves forward, the image is collected one line at a time, with all of the pixels in a line being measured simultaneously. Linear charge coupled device (CCD)/photodiode arrays (Fig. 2.8) generate images in this mode. The whisk broom or spotlight or across track scanners, on the other hand, use a mirror to reflect light onto a single detector. The mirror moves back and forth, to collect measurements from one pixel in the image at a time. One cross-track line of width equal to one pixel is imaged. Successive scan lines are produced by the motion of the platform (Fig. 2.9).

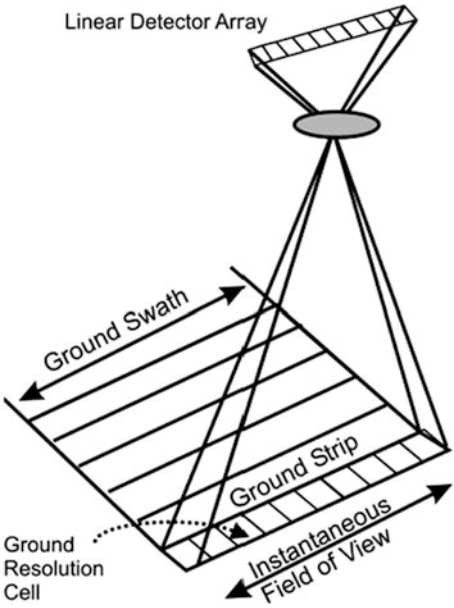

Fig. 2.7 Sketch of a push broom scanner

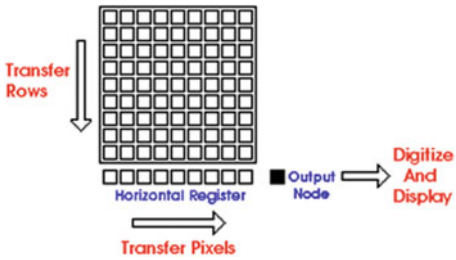

Fig. 2.8 Charge-coupled device

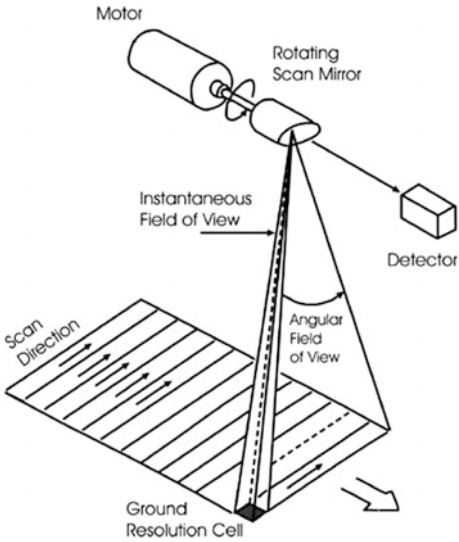

Fig. 2.9 Sketch of an opto-mechanical scanner

2.3.2 Microwave Sensors

Sensors operating in the microwave region of electromagnetic spectrum can be grouped into two categories namely active microwave sensors and passive microwave sensors. Active microwave remote sensors provide their own illumination, whereas passive systems measure the electromagnetic energy of thermal origin emitted from materials. A brief description of the sensors used in microwave remote sensing is given hereunder.

2.3.2.1 Passive Microwave Sensors

Passive microwave sensors are called radiometers and measure the emissive properties of the Earth's surface. A microwave radiometer is a sensitive receiver capable of measuring low levels of emitted microwave radiations from the surfaces under observation. The receiver consists, in principle, of a high-gain antenna,

switching device, one or several noise sources of known temperatures used as calibration reference, a band-pass filter, amplifier and a detector. The signal received at antenna is compared with the signals of the reference sources by switching between the antenna and input and the reference loads. The microwave radiometric measurements thus made can be expressed in terms of temperature (Eq. 2.1). The radiometric resolution, ΔT, characterizes the performance of a microwave radiometer which may be expressed in general form (Ulaby et al. 1981):

$$\Delta T = M/\sqrt{Bt}, \tag{2.2}$$

where $B = \Delta\nu$ is the bandwidth in HZ, t is the integration time in sec and M is the radiometric figure of merit, which is a constant for a given receiver configuration, depending upon its technical design.

Because of the low intensity comparatively broad bands are used for scanning microwave radiometers to obtain the radiometric resolution of the order of several tenths of a degree. The spatial resolution microwave radiometer can be defined as *half-power bandwidth*, $\beta 1/2$. For an antenna with a circular aperture the ideal half-power bandwidth in radian is given by

$$\beta 1/2 = \lambda/d, \tag{2.3}$$

where d is the aperture diameter. Due to practical limits on the physical size of antenna, the resolution of spaceborne scanning microwave radiometers is ≥ 10 km and varies with the wavelength λ. Imaging microwave radiometers apply either mechanical scanning mechanism with a rotating antenna or electronic beam steering. Conical scanning mechanisms enable constant incidence angle on the surface. As an example, the Special Microwave Sensor/Imager (SMS/I) on-board DMSP satellite covers a swath of 1000 km width. The elliptical IFOV varies from 69 km $\times$ 43 km at 19 GHZ to 15 km $\times$ 13 km at 85 GHZ (Schultz 2000).

2.3.2.2 Active Microwave Sensors

Active microwave sensors transmit electromagnetic waves towards the target; the reflected/scattered waves, incident on the receiver, are recorded and analysed in order to derive information on physical structure and dielectric properties of the target (Elachi 1987; Ulaby et al. 1982). Active microwave could be grouped into two categories: imaging microwave sensors and non-imaging microwave sensors The imaging radars represent the first category of active microwave sensors.

Imaging Radar

Imaging radars are divided into two categories, viz. real aperture and synthetic aperture systems. In the real aperture system, spatial resolution is determined by the actual beam width determined by the antenna size. Synthetic aperture system

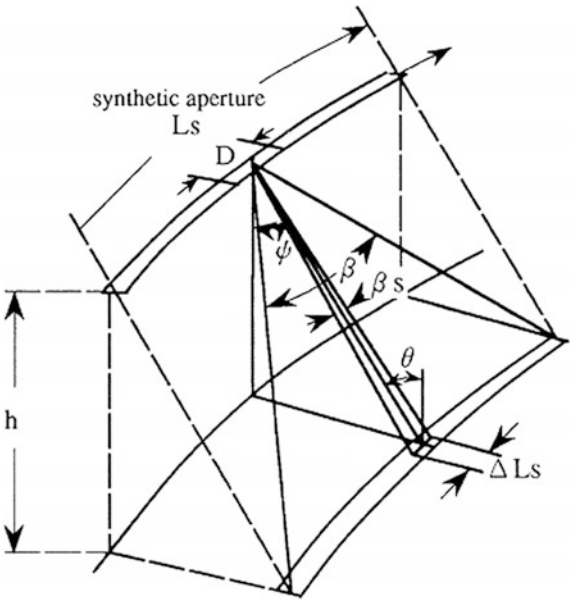

Fig. 2.10 Geometry of real aperture and synthetic aperture, radar. D real aperture, β real beam width, βs synthetic beam width, h height, ΔLs azimuth resolution and ψ off-nadir angle

utilizes signal processing techniques to achieve narrow beam width in the along-rack direction which provides better spatial resolution.

The geometry of real aperture radar is shown in Fig. 2.10. The microwave radiation is transmitted in the form of short pulse with duration Δt; the distance between the antenna and the target is calculated from the time difference between transmittance and reception of the pulse. The resolution in direction of the radar beam (the range resolution (R_r)) is calculated as follows:

$$R_r = c\tau/2, \tag{2.4}$$

where c is the speed of light (3×10^8 m/s) and τ is the pulse duration. c is slightly affected by atmospheric properties, in particular, water vapour content. For accurate range measurements (radar altimetry), these effects have to be corrected.

The range resolution is the slant range resolution. After accounting for depression angle (θ_d) effect, the ground resolution in the range direction is found from

$$R_r = \frac{c\tau}{2\cos\ \theta d}. \tag{2.5}$$

The azimuthal resolution in side-looking radar (SLR) system in azimuth, Ra, is determined by the angular beam width β of the antenna and the slant range SR (Fig. 2.11). The beam width of the antenna of a SLR system is directly proportional to the wavelength of the transmitted pulses, λ, and inversely proportional to the length of the ant antenna, D:

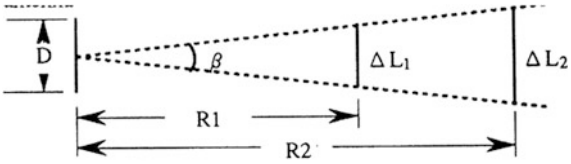

Fig. 2.11 Illustration of azimuth resolution of real aperture radar. β is the beam width, R1 and R2 are near and far ranges, respectively. ΔL1 and ΔL2 are azimuth resolutions at near and far ranges, respectively. (http://wtlab.iis.u-tokyo.ac.jp/~wataru/lecture/rsgis/rsnote/cp4/cp4-2.htm) Accessed on 25 July 2016

$$\beta = \frac{\lambda}{D}. \tag{2.6}$$

The azimuth resolution, ΔL, of SLR can be given as

$$\Delta L = \beta \cdot R = \frac{\lambda R}{D}. \tag{2.7}$$

However, as it is difficult to use such a large antenna, requiring, for example, a 1 km diameter antenna in order to obtain 25 m resolution with L-band (λ = 25 cm) and 100 km distance from a target, a real aperture radar therefore has a technical limitation for improving the azimuth resolution.

Non-Imaging Sensors

Non-imaging remote sensing radars are either scatterometers or altimeters. Any calibrated radar that measures the scattering properties of a surface is called scatterometer. Thus a scatterometer may be a radar specifically designed for backscatter measurements. The main application is a topographic mapping of ocean, lake and ice surfaces. *Scatterometers* measure accurately the surface backscatter across a swath of several hundred km width, but the spatial resolution is low. The main application is monitoring of wind velocity over the oceans which is derived from backscatter measurements. *Altimeters* are used for accurate surface height measurements along the satellite nadir track.

Radar Interferometry

In a quest to improve the accuracy of topographic maps, newer datasets, tools and techniques have been utilized. Aerial photographs and line-scanner images have been very often used as database for generating topographic maps. In aerial photographs and line-scanner imagery, the images of tops of objects are displaced from their bases and cause any object standing above the terrain to 'lean away' from the principal point of a photograph/satellite's nadir radially. This is called *relief displacement*. When an object is imaged from two different flight lines/orbits, differential relief displacements cause image *parallax*. This allows images to be viewed stereoscopically, and enables deriving information on terrain's elevation (z-axis) using photogrammetric technique.

Stereo radar images can be obtained by acquiring data from flight lines that view the terrain feature from opposite sides. However, because the radar side lighting will be reversed on the two images in the stereopair, stereoscopic viewing is somewhat difficult using this technique. Stereo radar imagery is, therefore, often acquired from two flight lines at the same altitude on the same side of the terrain feature. When a vertical feature is encountered by radar pulse, the backscattered energy from the top of the feature often reaches before the base. This will cause a vertical feature to 'layover' the closer feature, making it appear to lean towards the nadir. This layover effect is most severe at near range (steeper incidence angles). However, in contrast to scanner imagery and photography, the direction of relief displacement in radar images is reversed. This is because radar images display ranges or distances from terrain features to the antenna.

Imaging radar interferometry/SAR interferometry (InSAR) is based on the analysis of the phase of the radar signals as received by two antennas located at different positions in the space. As shown in Fig. 2.12, the radar signals returning from a single point on the Earth's surface will travel from slant range distance r1 and r2 to antenna A1 and A2, respectively. The difference between lengths r1 and r2 will result in the signals being out of phase by some phase difference (ǿ), ranging from 0 to 2π radians. If the geometry of the interferometric baseline (B) is known with a high degree of accuracy, this phase difference can be used to compute the elevation of point P.

As discussed in the preceding paragraph, the presence of differential relief displacement in overlapping radar images acquired from different flight lines produces image parallax. Just as photogrammetry can be used to measure surface topography and feature heights in optical images, radargrammetry can be used to make similar measurements in radar images.

There are several different approaches to collecting interferometric radar data. In the simplest case, referred to as *single-pass interferometry,* two antennas are located on a single aircraft or satellite platform. One antenna acts as both a transmitter and receiver, while another antenna acts only as a receiver. In this case as shown in

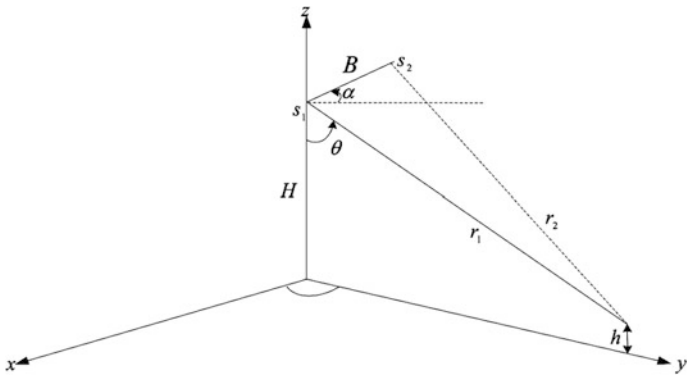

Fig. 2.12 Single-pass SAR interferometry

Fig. 2.13a the interferometric baseline is the physical distance between the two antennas. Shuttle Radar Topography Mission (SRTM) with a fixed-baseline interferometry mission is an example of *single-pass interferometry*.

Alternatively, in *repeat-pass interferometry*, an aircraft or satellite with only a single-radar antenna makes two or more passes over the area of interest, with antenna acting as both a transmitter and receiver on each pass. The interferometric baseline is then the distance between two flight lines or orbital tracks (Fig. 2.13b). It is generally desirable to have the sensor passes close as possible to its initial position, to keep this baseline small. For airborne repeat-pass interferometry, the flight lines should generally be separated by no more than tens of metres, while for spaceborne systems this distance can be as much as hundreds or thousands of metres.

In *repeat-pass interferometry*, the position and orientation of objects on the surface may change substantially between passes, particularly if the passes are separated by an interval of days or weeks. This results in a situation known as *temporal decorrelation* in which precise phase matching between the two signals is degraded. In some cases, repeat-pass interferometry can actually be used to study surface changes that have occurred between the two passes. In addition to 'before' and 'after' images, this approach—known as *differential interferometry*—also requires prior knowledge about the underlying topography. If the interferometric correlation between the two images is high, these changes can be accurately measured to within a small fraction of radar system's wavelength—often to less than 1 cm. When two interferometric radar datasets are combined, the first product

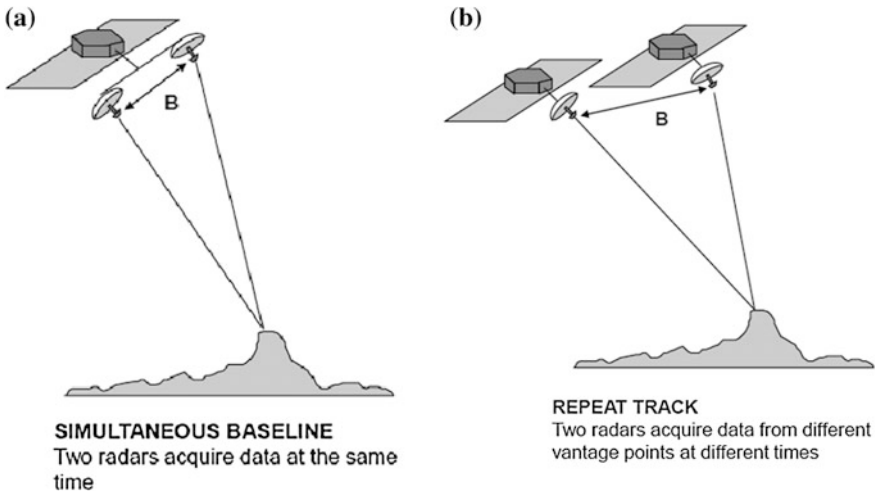

Fig. 2.13 **a** Single-pass interferometry (Simultaneous base line) **b** Repeat-pass interferometry (Repeat track baseline) (http://www.google.co.in/url?sa=t&rct=j&q=&esrc=s&source=web&cd=18&ved=0CEAQFjAHOAo&url=http%3A%2F%2Fwww.oregonstatehospital.net%2Fd%2Fotherfiles%2FInterferometry.pdf&ei=OAxjVLmUO8q9ugSDpIGwCw&usg=AFQjCNHyGAt8QE4dh6V3q0agd-qoGYYekQ&bvm=bv.79189006,d.c2E)

made is called an *interferogram* (also called a fringe map). A condition for interferogram is the preservation of the signal phase (coherence) between the two images. Coherence is affected by temporal changes of backscattering (due to snowmelt or rain). A fringe map looks similar to those bands of colour you see in a film (Fig. 2.14).

2.3.3 LiDAR

LiDAR (Light Detection And Ranging, also LADAR) uses ultraviolet, visible or near-infrared light to image objects and can be used with a wide range of targets, including nonmetallic objects, rocks, rain, chemical compounds, aerosols, clouds and even single molecule (Fig. 2.15). The fundamental concept of a LiDAR, also called LADAR, is to transmit a laser pulse towards a target and to measure the timing and amount of energy that is scattered back from the target. The return signal timing provides a measurement of the distance between the instrument and the scattering object (d):

$$t = 2d/c, \tag{2.8}$$

where c is the speed of light (299.79×10^6 m/s).

The major components of a LIDAR system include (i) laser, (ii) scanner and optics, (iii) photodetectors and receiver electronics, and (iv) position and navigation systems (Global Positioning System—GPS), and an Inertial Navigation System

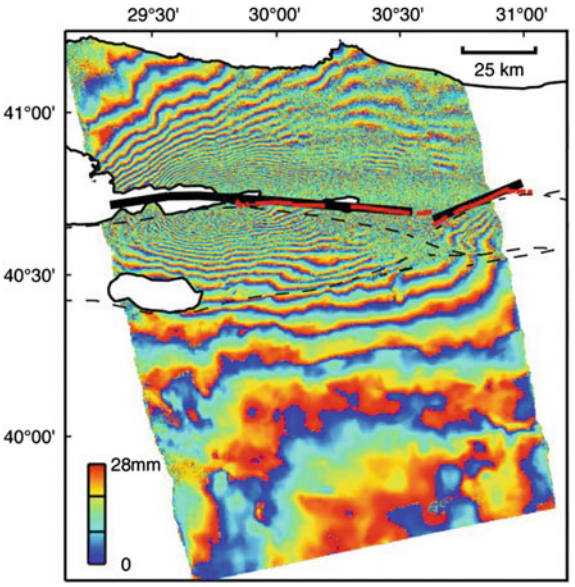

Fig. 2.14 Interferogram produced using ERS-2 data from 13 August and 17 September 1999, spanning the 17 August Izmit (Turkey) earthquake (NASA/JPL-Caltech) (http://en.wikipedia.org/wiki/Interferometric_synthetic_aperture_radar)

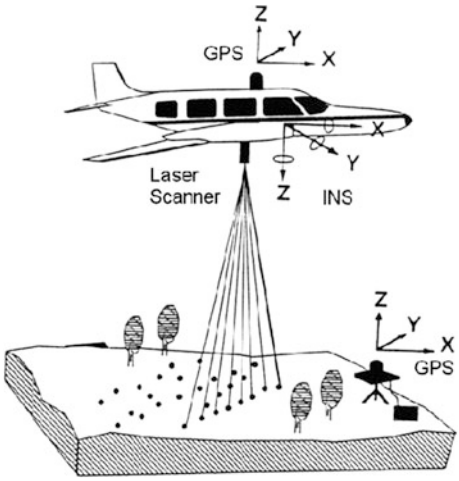

Fig. 2.15 An airborne LiDAR system

(INS). Depending upon the mode of capturing backscattered energy, there are broadly two types of LiDAR as shown in Fig. 2.16.

Discrete-return LiDAR In a discrete-return scanning LiDAR system, a laser pulse is sent out from the sensor and the leading edge of the returned signal trips a response for a time measurement. For many modern systems, the trailing edge of the response is also used to trip a second return time. These are referred to as the 'first' and 'last' returns. If the first return happens to be associated with a tree canopy top and the last return the underlying ground, then this single signal can be used to provide a measurement of tree height.

Waveform LiDAR In a waveform LiDAR, the system samples and records the energy returned for equal time intervals ('bins'). There are currently only a few such

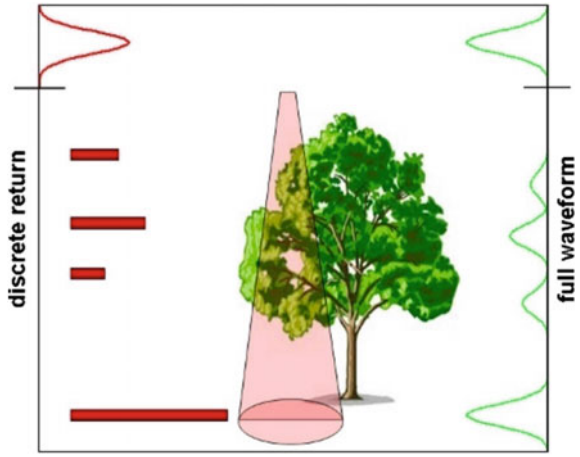

Fig. 2.16 Observational differences between discrete-return and full-waveform LiDAR

airborne systems and fewer still spaceborne instruments. Waveform LiDAR systems typically have a much larger footprint than discrete-return systems, being of the order of 10 s of metres. This is fundamentally for signal-to-noise reasons: the quantity of backscattered energy in a small field of view is low. The energy received per unit time bin is even smaller, so the sensor technologies need to be capable of measuring very low signal levels, very quickly. The LiteMapper-5600 system quotes a waveform sampling interval of 1 ns, giving a multi-target resolution (related to bin size) of better than 0.6 m (Hug et al. 2004).

In general there are two kinds of LiDAR detection schema: "incoherent" or direct energy detection, which is basically an amplitude measurement, and coherent detection (which is best for Doppler, or phase sensitive measurements). Coherent systems generally use optical heterodyne detection which being more sensitive than direct detection allows them to operate a much lower power but at the expense of more complex transceiver requirements.

In both coherent and incoherent LiDARs, there are two types of pulse models: micropulse lidar systems and high-energy systems. Micropulse systems use considerably less energy in the laser, typically on the order of one microjoule, and are often "eye-safe", meaning they can be used without safety precautions. High-power systems are common in atmospheric research, where they are widely used for measuring many atmospheric parameters: the height, layering and densities of clouds, cloud particle properties (extinction coefficient, backscatter coefficient, depolarization), temperature, pressure, wind, humidity and trace gas concentration (ozone, methane, nitrous oxide, etc.) (http://carms.geog.uvic.ca/LiDAR%20Web%20Docs/LiDAR%20paper%20june%202006.pdf; http://classes.css.wsu.edu/soils374/ppt/lidar2.pdf and http://www.softree.com/articles/LiDARWorkshop.pdf).

2.4 The Ground Segment

The ground segment is an integral part of the remote sensing system. A satellite is not just put into orbit and left alone. Even at the height of most low-Earth orbits there will be some atmospheric drag on a satellite and, left to itself, the satellite's orbit would decay and it would eventually burn up in the denser atmosphere. Also, any slight perturbation may affect the satellite's stability and it would eventually start spinning. Ground control will therefore constantly monitor the conditions and take steps to rectify such problems by firing on-board rockets to boost the orbit and to make sure the detector is pointing in the direction required. Ground control will also control the post-launch deployment of solar panel and antennae and commission the on-board instruments. It will constantly monitor the performance of the instruments and take such action as is necessary to remedy any problems, often by reprogramming of switching circuits (Hamlyn and Vaughan 2010).

For any satellite remote sensing system, some means of transferring the information that has been gathered by the sensors on the satellite back to the Earth is necessary. In the case of a manned spacecraft, the recorded data can be brought

back by the astronauts in the spacecraft when they return to Earth. However, the majority of scientific remote sensing data gathered from space is gathered using unmanned spacecraft. The data from an unmanned spacecraft must be transmitted back to Earth by radio transmission from the satellite to a suitably equipped ground station. The transmitted radio signals can only be received from satellite when it is above the horizon of the ground station. In the case of polar-orbiting satellites, global coverage could be achieved by having on-board data recorder(s) and transmitting the recorded data back to Earth when satellite is within the range of a ground station. However, in practice, it is only possible to provide tape recording facilities adequate for recording a small fraction of the data that could, in principle, be gathered during each orbit of the satellite. Alternatively, global coverage could be made possible by (i) having a network of receiving stations suitably distributed over the globe, or (ii) by using geostationary satellites for linking the signals from an orbiting remote sensing satellite with a receiving station at all times (Cracknell and Hays 2007).

2.5 Earth-Observing Systems (EOS)

For imaging, the Earth sensors operating both in optical and microwave region of the electromagnetic spectrum have been developed and flown aboard various Earth observation missions. Presented hereunder is a brief overview of some of the important Earth observation satellites carrying optical as well as microwave sensors.

2.5.1 The Landsat System

The Landsat system was the first civil Earth-observing satellite programme. It began with the launch of the first Landsat satellite in 1972 and has been continuing with the Landsat-8 mission launched in 2013. For over four decades, the Landsat programme has continuously collected spectral information from Earth's surface. Since June 2009, the entire Landsat image archive is available at no charge online. Further details of the Landsat system are available at https://directory.eoportal.org/web/eoportal/satellite-missions/l/landsat-1-3.

2.5.1.1 The First Landsat Series

The first three satellites of Landsat series (Landsat-1, -2 and -3) were identical and their payloads consisted of two optical instruments, a multispectral sensor (Multi spectral Scanner or MSS) and a series of video cameras (Return Beam Vidicons or RBVs). Landsat-1 was launched on 23 July 1972 and was operational up

to 6 January, 1978. Landsat-2 had operated during January 1975 to 5 February, 1982 whereas Landsat-3 had been functional during 5 March, 1978 to 31 March, 1983.

Return Beam Vidicon (RBV) sensors The payloads of the first two Landsats included a series of three video cameras that took pictures in the visible and infrared bands—band1 (0.48–0.58 μm), band2 (0.58–0.68 μm) and band3 (0.70–0.83 μm). The spatial resolution was 80 m with a swath width of 185 km. The resolution of the images acquired by Landsat-3 was raised to 40 m, but the cameras took images in a single panchromatic spectral band (0.5–0.75 μm) only.

Multi-spectral Scanner or (MSS) Sensors These opto-mechanical sensors collected images of the Earth in four spectral bands: band4 (0.5–0.6 μm), band5 (0.6–0.7 μm), band6 (0.7–0.8 μm) and band7 (0.8–1.1 μm) over a swath of 185 km. Since this instrument was developed after the three RBV cameras, these bands were numbered from 4 to 7. Multispectral scanner on-board Landsat-3 included an additional spectral band in the thermal infrared band (10.4–12.6 μm) with a spatial resolution of 240 m.

2.5.1.2 The Second Landsat Series

The next two satellites (Landsat-4 and -5) were equipped with two multispectral sensors, i.e., a multispectral scanner (MSS) and a Thematic Mapper (TM). Whereas Landsat-4 was launched on 16 July, 1982 and had operated till July 1987, the operational duration of Landsat-5 was pretty long—1 March, 1985 to 5 June, 2013 (http://en.wikipedia.org/wiki/Landsat_program). The multispectral scanners (MSSs) on-board Landsat-4 and 5 were identical to those on the first three Landsat satellites except for the four spectral bands numbered from 1 to 4 since the RBVs were no longer used. Landsat-5's MSS stopped acquiring data in 1992. Thematic mappers (TMs) aboard Landsat-4 and -5 were, in fact, state-of-the-art sensors with seven spectral bands spanning from visible-IR (blue: 0.45–0.52 μm; green: 0.52–0.60 μm; red: 0.63–0.69 μm) through near-IR (0.76–0.90 μm), shortwave-IR (1.55–1.75; 2.08–2.35 μm) and thermal IR (10.4–12.5 μm) regions of the spectrum, and improved spatial resolution (30 m) and radiometric resolution (8bit) which were dedicated to specific applications.

2.5.1.3 The Third Landsat Series

The last generation of Landsat satellites comprises Landsat-6, -7 and -8 missions. The Landsat-6 was lost just after its launch on 3 October 1993. Landsat-7 was launched on 15 April, 1999 and is equipped with a multispectral sensor known as the Enhanced Thematic Mapper Plus (ETM+). The observation bands are essentially the same seven bands as TM, and a panchromatic band 8 (0.5–0.90 μm) with 15 m

spatial resolution has been added. Two key components of the ETM+ optical system are the rotating scanning mirror and the scan line corrector (SLC). The mirror provides cross-track imaging coverage while the satellite's forward velocity provides along-track coverage. The SLC removes the zig-zag effect caused by the combined along-track and cross-track motions (Fig. 2.17). An instrument malfunction occurred on 31 May, 2003, with the result that all Landsat 7 scenes acquired since 14 July, 2003 have been collected in "SLC-off" mode (Fig. 2.10).

Landsat-8 was launched on 11 February, 2013 to ensure the continuity of Landsat-like data well beyond the duration of the current Landsat-7 mission. Initially christened as Landsat Data Continuity Mission (LDCM), it was renamed later as Landsat-8. Landsat-8 has two sensors, namely Operational Land Imager (OLI) and Thermal Infrared Sensor (TIS) on-board.

Operational Land Imager (OLI) The Operational Land Imager (OLI) is a push broom sensor with a four-mirror telescope and 12-bit quantization level. It collects image data for nine shortwave spectral bands over an 185 km swath with a 30 m spatial resolution for all bands spanning from 0.43 to 2.29 μm, except a 15 m panchromatic band. The OLI also collects data for two new bands, a coastal band (0.43–0.45 μm) and a cirrus band (1.36–1.38 μm), as well as the heritage Lands at

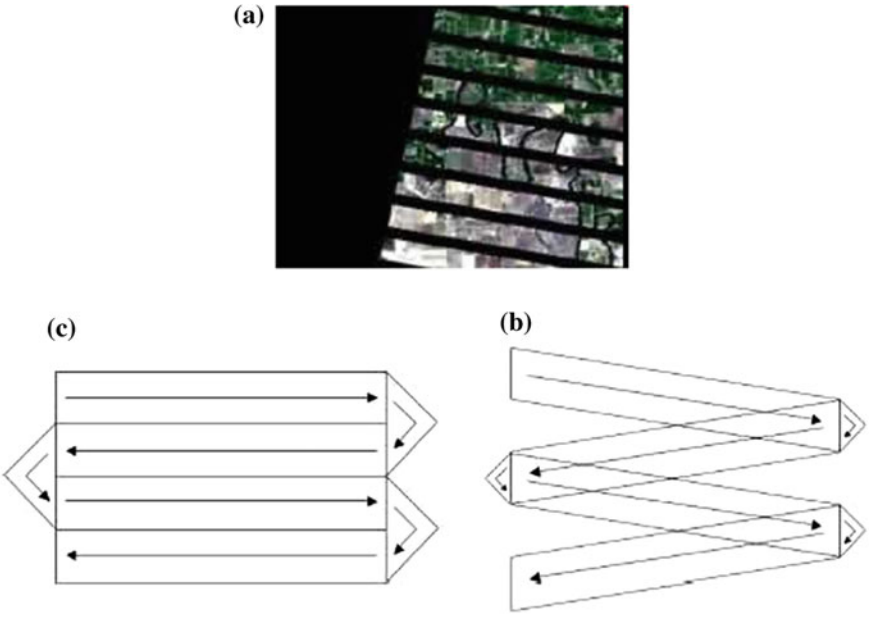

Fig. 2.17 Showing the effect of malfunctioning of scan line corrector (SLC) **a** Sketch of part of the uncorrected image (**b**) and after correction. **b** The effects of scan line corrector (SLC) malfunction on image quality. Data gaps produced from the SLC-off mode have alternating wedges with the widest parts occurring at the scene edge. *Source* http://www.gis.unbc.ca/wp-content/uploads/2013/05/correction.pdf accessed on 19 July 2016

Table 2.1 Salient features of Landsat-8 sensors

Spectral channel	Wavelength (μm)	Spatial resolution (m)
Operational land imager (OLI) spectral channels		
Band 1	0.43–0.45	30
Band 2	0.45–0.51	30
Band 3	0.53–0.59	30
Band 4	0.64– 0.67	30
Band 5	0.85–0.88	30
Band 6	1.57–1.65	30
Band 7	2.11–2.29	30
Band 8 (PAN)	0.50–0.68	15
Band 9 (Cirrus)	1.36–1.38	30
Thermal Infrared Sensor (TIRS)		
Band 10	10.6–11.19	100
Band 11	11.5–12.51	100

Source http://landsat.gsfc.nasa.gov/about/ldcm.html

multispectral bands. Additionally, the bandwidth has been refined for six of the heritage bands (Table 2.1).

Thermal Infrared Sensor (TIRS) The Thermal Infrared Sensor (TIRS) was added to the Landsat-8 payload to continue thermal imaging and to support emerging applications such as evapotranspiration rate measurements for water management. The 100 m TIRS data could be registered to the OLI data to create radiometrically, geometrically and terrain-corrected 12-bit LDCM data products.

2.5.1.4 Multi-sensor Formation Concept

Since a single sensor cannot make all desired measurements of the Earth and its atmosphere, we must rely on combining data from several sensors to achieve the complete picture for scientific analysis. One of the ways to do this is to create a 'train' of sensors on different satellites travelling in the same orbit and separated by short time intervals similar to the planes flying in formation. The initial NASA's demonstration of this concept was a morning formation, including Landsat-7 in the lead, EO-1 (1 min behind Landsat-7), Terra (15 min behind) and the Argentine satellite SAC-C (30 min behind). These satellites all descend across the equator on the daylight side of the Earth in the morning as shown in Fig. 2.18. The afternoon A-Train was established later with Aqua in the lead, followed by several atmospheric sensors satellites including CloudSat (1 min behind Aqua) and CALIPSO (2 min behind) all in an ascending orbit.

Depending on the application, there are three formations possible: trailing, cluster and constellation.

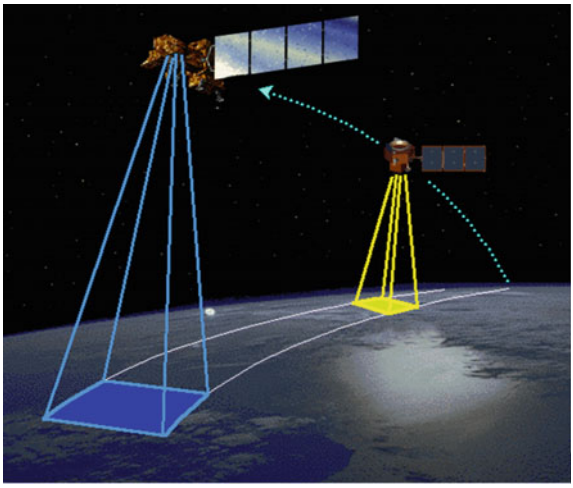

Fig. 2.18 Landsat-7 being trailed by EO-1 covering the same area at different times

Trailing formations are formed by multiple satellites orbiting on the same path. They are displaced from each other at a specific distance to produce either varied viewing angles of one target or to view a target at different times. Trailing satellites are especially suited for meteorological and environmental applications such as viewing the progress of a fire, cloud formations, and making 3D views of hurricanes. Notable pairs are Landsat 7 with EO-1, the "A-train" consisting of CALIPSO and CloudSat (among others), and Terra with Aqua.

Cluster formations are formed by satellites in a dense (relatively tightly spaced) arrangement. These arrangements are best for high-resolution interferometry and making maps of Earth. TechSat-21 was a suggested satellite model capable of operating in clusters (http://en.wikipedia.org/wiki/Satellite_formation_flying) accessed on 30 November 2014. A *satellite constellation* is a group of artificial satellites working in concert. Such a constellation can be considered to be a number of satellites with coordinated ground coverage, operating together under shared control, synchronized so that they overlap well in coverage and complement rather than interfere with other satellites' important coverage. The constellation of satellites in the Global Navigation Satellite System (GNSS) is a typical example (http://en.wikipedia.org/wiki/Satellite_constellation) accessed on 30 November 2014.

2.5.2 *Satellite Pour l'Observation de la Terre (SPOT)*

The SPOT system is the second-generation Earth-observing systems. The SPOT satellites constellation offers acquisition of images of the Earth from anywhere in

the world, every day above 40° N and 40° S latitude any point, whatsoever can be observed each day of the year.

2.5.2.1 The First SPOT Series

The first three SPOT satellites (SPOT-1, -2 and -3) were identical, and their payloads consisted of two identical HRV (Visible High-Resolution) optical instruments (Fig. 2.19). Each HRV can operate simultaneously or individually in either panchromatic (0.50–0.73 μm) mode or multispectral mode in three spectral bands, viz. the green (0.50–0.59 μm), red (0.61–0.68 μm) and infrared (0.78–0.89 μm) band. Whereas the spatial resolution of multispectral HRV sensor was 20 m, the panchromatic band acquired images with 10 m resolution. The orientation of each

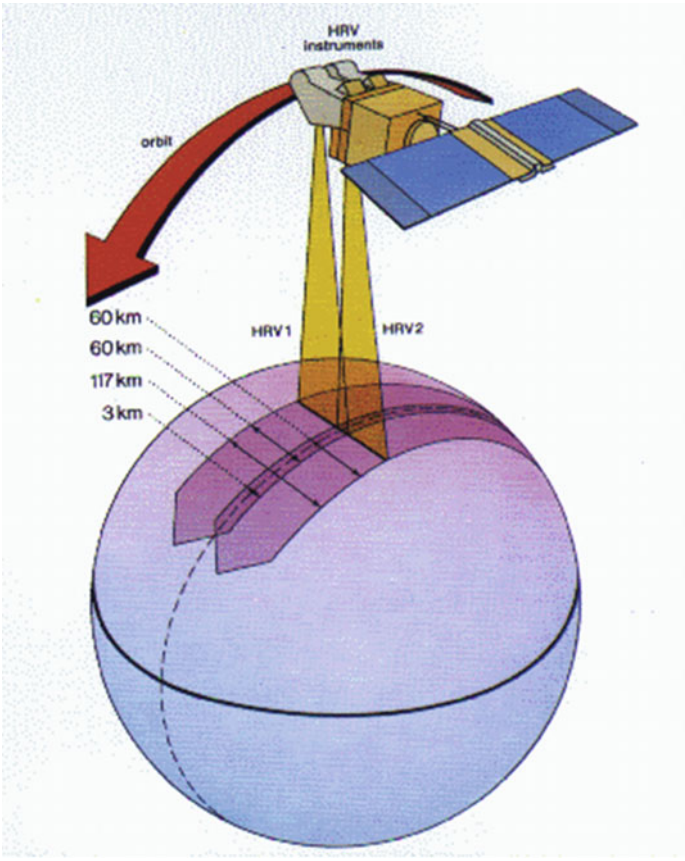

Fig. 2.19 SPOT 1, 2 twin HRV (SPOT 4 twin HRVIR) imaging system. *Source* https://www.google.co.in/?gws_rd=ssl#q=spot-4+satellite+High+Resolution+Vertical+Infrared+%28HRV-IR

instrument's strip selection mirror can be remotely steered by the ground stations, offering an oblique viewing capability up to angles of ±27° from the satellite's vertical axis. In this way, the temporal resolution is shortened from 26 to 4–5 days for the temperate zones. SPOT-1 was launched on 21 February, 1986 and operated successfully till 1 November, 2003. Whereas SPOT-2 operated during the period 21 January, 1990 to 30 June, 2009, SPOT-3 acquired images of the Earth only for a period of over 3 years (25 September, 1993 to 14 November, 1996). Its unique features are the use of linear array (also called push broom) detectors (Fig. 2.20) and the off-nadir observation capabilities with the HRV sensors as shown in Fig. 2.21.

The SPOT sensors can also acquire cross-track stereoscopic pairs of images for a given geographic area (Fig. 2.19). The observations can be made on successive days such that the two images are acquired at angles on either side of the vertical. In such cases, the ratio between the observation base (distance between the two satellite positions) and the height (satellite altitude) is approximately 0.75 at the equator and 0.50 at a latitude of 45°. Tests have shown that SPOT data with these base-to-height ratios may be used for topographic mapping. Toutin and Beaudoin (1995) applied photographic techniques to SPOT data and produced maps with a planimetric accuracy of 12 m with 90% confidence.

2.5.2.2 The Second SPOT Series

This series consists of two satellites (SPOT-4 and -5) with improved payloads. The payload of SPOT-4 consists of two identical Visible and Infrared High-Resolution

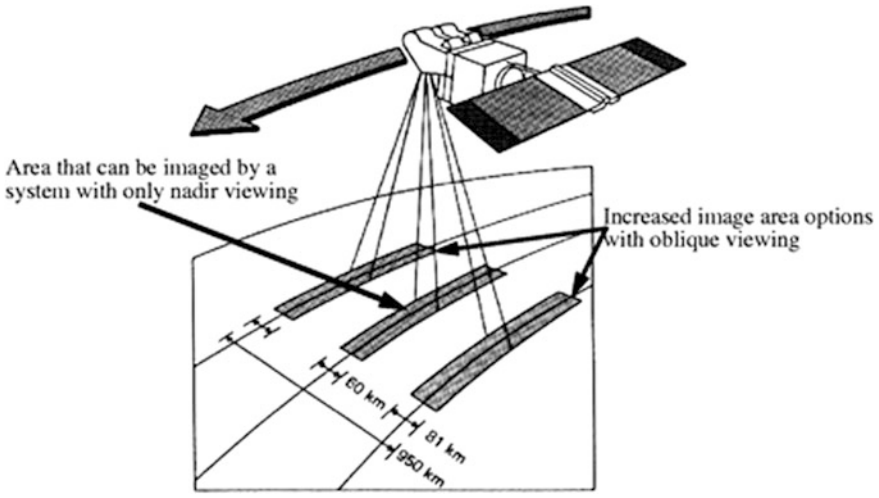

Fig. 2.20 Off-nadir viewing capability of SPOT HRV, HRVIR enables a short revisit interval of 1–3 days. *Source* http://www.crisp.nus.edu.sg/~research/tutorial/spot.htm (Accessed on 27 November 2014)

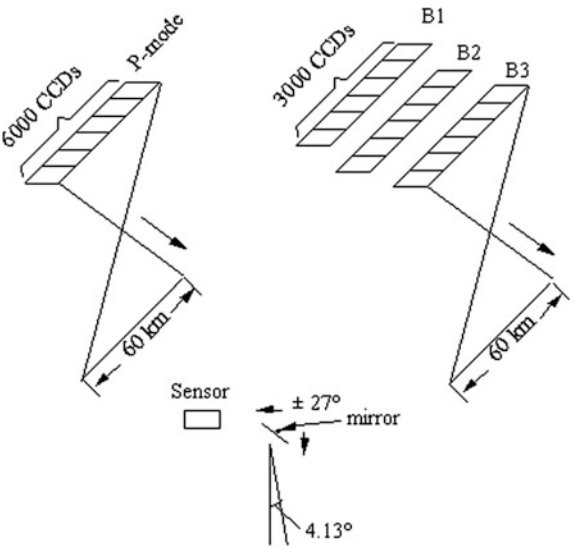

Fig. 2.21 The schematic diagram of the HRV CCD arrays in panchromatic B&W modes of data acquisition

(HRVIR) optical sensors and the VEGETATION sensor. The HRVIR sensors are similar to the HRV sensors of the previous generation. However, they differ by:

(i) the presence of an additional spectral band in the middle-infrared band (1.58–1.75 μm);
(ii) the panchromatic (0.51–0.73 μm) band's being replaced by the B2 (0.61–0.68 μm) band, which can function equally well in '10 m' and '20 m' mode; and
(iii) on-board superimposition of all of the spectral bands.

Because the SPOT-4 HRV sensors are sensitive to a SWIR band they are referred to as High-Resolution Visible IR (HRVIR). The SPOT VEGETATION sensors are completely independent of the HRVIR sensors. It is a multispectral electronic scanning radiometer operating at optical wavelength with a separate objective lens and sensor for each of the four spectral bands; blue (0.43–0.47 μm) used primarily for atmospheric correction; red (0.61–0.68 μm); near-infrared (0.78–0.89 μm); and SWIR (1.58–1.75 μm). Each sensor takes the form of a 1728 CCD linear array located in the focal plane of the corresponding objective lens. The VEGETATION sensor has a spatial resolution of 1.15 km. The objective lenses offer a field of view of ±50.05° which translates into a 2250 km swath width.

- *SPOT-5 High-Resolution Geometric (HRG) Sensors* There are two HRG sensors which capture the images of the Earth in green, red, near-IR with 20 m spatial resolution panchromatic images with 5 m resolution and in super mode 2.5 m panchromatic images. The swath width 60 km, same as its predecessors.

- *HRS Sensors* This is an instrument with the ability to acquire stereo pair images simultaneously, a considerable advantage for the quality of digital elevation model (DEM) production. The sensor is capable of providing 10 m spatial resolution with along the track sampling interval of 5 m. The swath with width of the sensor centred on the satellite track of 120 km with a viewing angle of ±20°. The VEGETATION sensor is same as in case of SPOT-4 mission.

2.5.2.3 The Third SPOT Series

Like previous series it also consists of two missions, viz. SPOT-6 and -7. SPOT-6 was launched on 9 September, 2012 and SPOT 7 on 30 June 2014 from Satish Dhawan Space Centre, Sriharikota, Andhra Pradesh, India. SPOT-6 and -7 are two agile Earth observation satellites to continue the services of the SPOT-4 and -5 missions. Both satellites offer 2 m resolution data in a 60 km by 60 km swath. The satellites will be co-orbital with the high-resolution Pléiades-HR satellites. The 1.5-metre-resolution natural-colour products, orthorectified as standard product and daily revisits to any point on the globe are the significant improvements in the SPOT- 6 and SPOT-7 missions. With location accuracy better than 10 m (CE90) and a resolution of 1.5 m, SPOT-6 and SPOT-7 are the ideal solution for national 1:25,000 scale map series (http://www.astrium-geo.com/en/147-spot-6-7-satellite-imagery). Operating in both panchromatic (0.450–745 nm) with 1.5 m spatial resolution, and multispectral (450–525; 530–590; 625–695 and 760–890 nm) mode simultaneously, the sensor provides 1.5 and 6 m spatial resolution, respectively.

Automatic ortho-image with a location accuracy of 10 m CE90 uses Reference 3D 120 km × 120 km bi-strip or 60 km × 180 km tri-strip mapping in a single pass and delivery of mosaic product stereo and tri-stereo acquisition of 60 km 60 km scenes for production of DEM 6 tasking plans per day (http://www.satimagingcorp.com/satellite-sensors/spot-6/) and (http://www.itc.nl/research/products/sensordb/getsat.aspx?name=SPOT%207). The SPOT-7 satellite is identical to SPOT-6, which was deployed by another PSLV launch in September 2012. Two imaging systems aboard the spacecraft, the New AstroSat Optical Modular Instruments (NAOMI), are capable of producing panchromatic images at a resolution of 1.5–2.2 m, and multispectral images at a resolution of 6.0–8.8 m. These instruments can cover a swath of 60 kms (http://www.nasaspaceflight.com/2014/06/indias-pslv-successfully-lofts-spot-7-companions/).

2.5.3 PLÉIADES Systems

The Pleiades-1A satellite is capable of providing orthorectified colour data at 0.5 m resolution (roughly comparable to GeoEye-1) and revisiting any point on Earth as it covers a total of 1 million square kilometres (approximately 386,102 square miles)

daily. Perhaps most importantly, Pleiades-1A is capable of acquiring high-resolution stereo imagery in just one pass, and can accommodate large areas (up to 1000 km × 1000 km). The Pleiades-1A satellite features four spectral bands (blue, green, red and IR), as well as image location accuracy of 3 m (CE90) without ground control points. Image location accuracy can be improved even further—up to an exceptional 1 m by the use of GCPs. Because the satellite has been designed with urgent tasking in mind, images can be requested from Pleiades-1A less than six hours before they are acquired. This functionality will prove invaluable in situations where the expedited collection of new image data is crucial, such as crisis monitoring (http://www.satimagingcorp.com/satellite-sensors/pleiades-1/) accessed on 30 November 2014.

Pléiades systems consist of Pléiades 1A and Pléiades 1B. Pléiades 1A was launched on 16 December, 2011 whereas Pléiades 1B on 2 December, 2012. With identical sensors the two satellites are operating in the same phased orbit and are offset at 180° to offer a daily revisit capability over any point on the globe. The ground resolution is 50 cm in panchromatic (480–830 nm) mode, and 2 m in multispectral (blue: 430–550 nm; green: 490–610 nm; red: 600–720 nm and near-infrared: 750–950 nm) mode across a 20 km swath, while a very high degree of agility allows them to acquire several images successively along track or off track, for preparing mosaicks of ground scenes.

In addition to their high precision, the Pleiades-1 satellites are also notable for their remarkable agility, which enables tilted imaging from nadir and operation in several acquisition modes (20 images over 1000 × 1000 km^2, stereo, 3D, mosaic, corridor, etc.) (http://www.satimagingcorp.com/satellite-sensors/pleiades-1/) accessed on 30 November 2014.

2.5.4 The Indian Remote Sensing Satellites (IRS) Mission

Consequent upon the successful launch of Bhaskara-1 and Bhaskara-2 in 1979 and 1981, respectively, India began to develop indigenous, viz. Indian Remote Sensing Satellite (IRS) programme to support the natural resources and environmental management. The orbital pattern of IRS series of satellites is shown in Fig. 2.22. A brief overview of the IRS mission is presented hereunder.

2.5.4.1 The IRS Series of Satellites

The first satellite in the Indian Remote Sensing (IRS) series-IRS-1A was launched on 17 March, 1988 carrying two sensors, viz. Linear Imaging Self-scanning Sensors (LISS-I and II) with 72.5 m 36.25 m spatial resolution and 146 km swath (Table 2.2). The repetivity of observation was 22 days. It was followed by the launch of its backup satellite, namely IRS-B in 1991 (August 29, 1991) with similar sensors. The IRS-P1 (also -1E) and IRS-P2 were launched in 1993 and 1994,

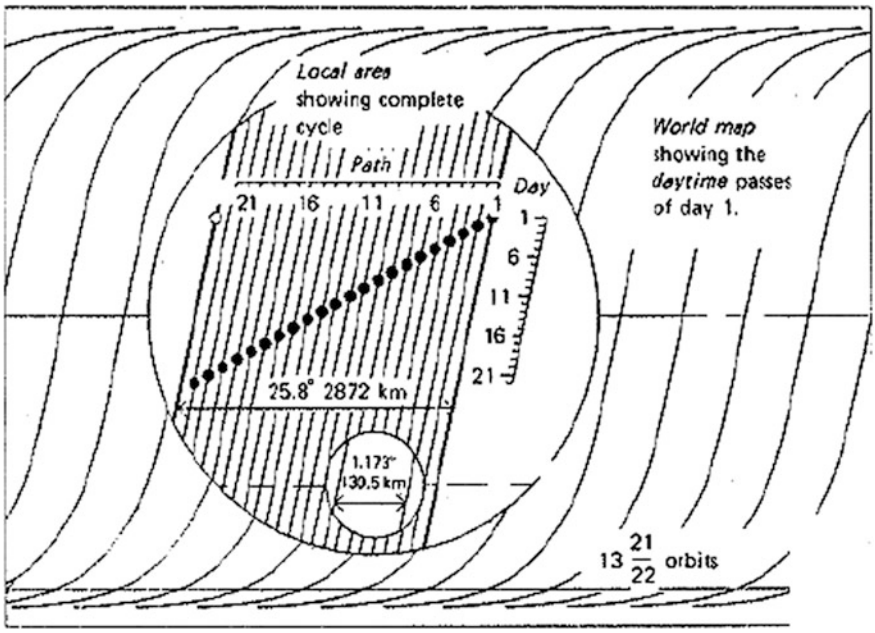

Fig. 2.22 Indian remote sensing satellite orbital coverage pattern

respectively. The major thrust to India's Earth observation from space came from the launch of IRS-1C in December 1995 with three sensors, viz. Wide Field Sensor (WiFS), Linear Imaging Self-scanning Sensor (LISS-III) and a panchromatic sensor (PAN). While LISS-III provides a spatial resolution of 23.5 m with a swath of 146 km, WiFS offers only 180 m spatial resolution (Table 2.2). The panchromatic sensor (PAN) provides a spatial resolution of 5.8 m. The launch of IRS-1D with similar sensors as of IRS-1C in 1997 marked the continuity of the latter mission. One more satellite, namely IRS-P3, was added in the IRS series in 1996. All the above-mentioned missions were dedicated to land observation.

Due emphasis was, however, laid on ocean observation too by launching the IRS-P4 (Oceansat-1) on 26 May, 1999 with two sensors, namely Ocean Colour Monitor (OCM) and a Multi-frequency Scanning Microwave Radiometer (MSMR) for oceanographic studies. The major characteristics of the optical sensors of IRS series (land observation) of satellites is given in Table 2.3.

2.5.4.2 Resourcesat-1

Resourcesat-1 was launched in 17 october, 2003 with three unique sensors, viz. Advanced Wide Field Sensor (AWiFS), LISS-III and LISS-IV offer immense potential in deriving regional, macro- and micro-level information on natural resources and environment, respectively (Fig. 2.23). There is a provision for

Table 2.2 Salient features IRS series of satellite sensors

Sensor	Resolution (m)	SwathWidth (km)	Spectral Bands (μm)
Linear imaging self-scanning sensor (LISS-I)	72	148	0.45–0.52 0.52–0.59 0.62–0.68 0.77–0.86
Linear imaging self-scanning sensor (LISS-II)	36	74	0.45–0.52 0.52–0.59 0.62–0.68 0.77–0.86
Linear imaging self-scanning sensor (LISS-III)	23 50	142 148	0.52–0.59 0.62–0.68 0.77–0.86 1.55–1.70
	6	70	0.5–0.75 (PAN)
Linear imaging self-scanning sensor (LISS-IV)	5.8	24–70	0.52–0.59 0.62–0.68 0.77–0.86
Wide field sensor (WiFS)	188	774	0.62–0.68 0.77–0.86
Advanced wide field sensor (AWiFS)	56–70	370–740	0.52–0.59 0.62–0.68 0.77–0.86 1.55–1.70

http://uregina.ca/piwowarj/Satellites/IRS.html (Accessed on 8 January 2015)

Table 2.3 Salient features of Resourcesat-2 sensors

Specifications	AWiFS	LISS-III	LISS-IV
No. of bands	4	4	1 (mono), 3 (MX)
Spectral bands (μm)	B2 0.52–0.59 B3 0.62–0.68 B4 0.77–0.86 B5 1.55–1.70	B2 0.52–0.59 B3 0.62–0.68 B4 0.77–0.86 B5 1.55–1.70	B2 0.52–0.59 B3 0.62–0.68 B4 0.77–0.86 B5 1.55–1.70 B3-default band for mono
Spatial resolution (m)	56	23.5	5.8
Swath (km)	740	140	70/23
Revisit (days)	5	24	5
Datarate (Mbs per stream)	105	105	105
Quantization	12-bit	10-bit	10-bit

Source http://lps16.esa.int/posterfiles/paper1213/[RD13]_Resourcesat-2_Handbook.pdf

recording data for any part of the world with its on-board solid-state recorder with 120 GB capacity. Additionally, by virtue of larger swath (740 km) and very high respectively (5 days) AWiFS also enables monitoring certain highly dynamic phenomenon like drought, flood, vegetation vigour, etc. An improved version of LISS-III with 4 spectral bands (red, green, near-IR and SWIR), all at 23 m spatial

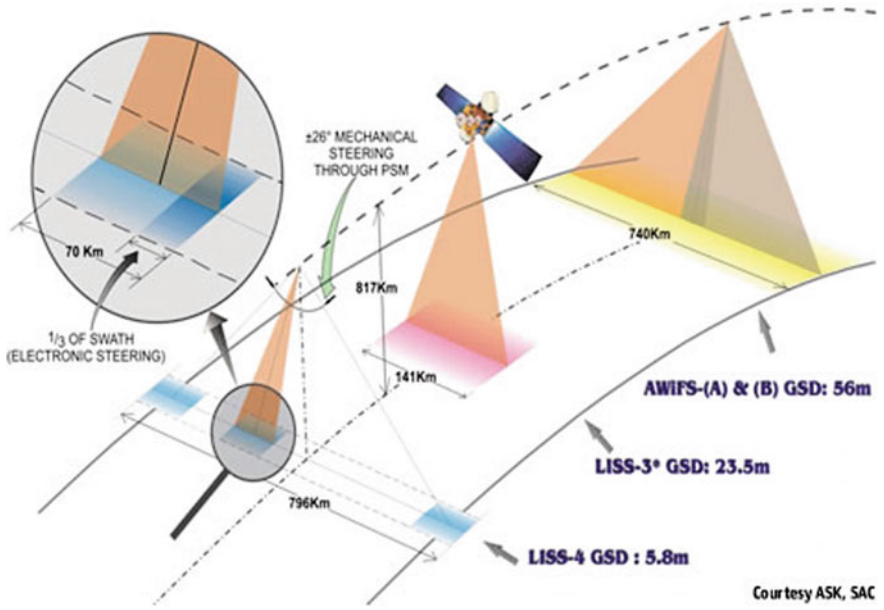

Fig. 2.23 Resourcesat-1 imaging modes http://www.angelfire.com/co/pallav/sensorindian.html (Accessed on 08 January 2015)

resolution and 140 km swath, provide the continuity to LISS-III data. The LISS-III has a receptivity of 24 days.

Advanced Wide Field Sensor (AWiFS) Advanced Wide Field Sensor (AWiFS) is an improved version of WiFS flown aboard IRS-1C/-1D missions. AWiFS operates in four spectral bands identical to WiFS with 10bit radiometry and a spatial resolution of 56 m covering a swath of 740 km. It has a 5-day revisit capability for 80% of the area covered. AWiFS is extremely useful in species-level vegetation mapping, sub-district level agricultural drought assessment and integrated land and water resources-related applications.

The LISS-III sensor is identical to the LISS-III sensor flown aboard IRS-1C/-1D spacecrafts except that the spatial resolution of shortwave infrared (SWIR) band (B5 1.55–1.75 μm) has been improved from 70.5 m in case of IRS-1C/-1D to 23.5 m. The Linear Imaging Self-scanning Sensor (LISS-IV) is a high-resolution multispectral sensor operating in three spectral bands, viz. B2 (0.52–0.59 μm), B3 (0.62–0.68 μm) and B4 (0.77–0.86 μm). LISS-IV provides a spatial resolution of 5.86 m (at nadir) and can be operated in two modes: multispectral and mode. In multispectral mode it covers a swath of 23 km selectable from 70 km of total swath in three bands. In monomode (panchromatic mode) the full swath of 70 km is covered in one single band which is selectable by ground command. LISS-IV can be tilted up to ±26° in the across track direction thereby providing a revisit period of 5 days. The oblique viewing (off-nadir viewing) capability can be used to acquire stereo pairs in monomode only.

2.5.4.3 Resourcesat-2

To maintain the continuity of remote sensing data services to global users provided by Resourcesat-1, and to provide data with enhanced multispectral and spatial coverage as well, Resourcesat-2 was launched on 20 April, 2011 as a follow-on mission to Resourcesat-1. Important changes in Resourcesat-2 compared to Resourcesat-1 are enhancement of LISS-IV multispectral swath from 23 to 70 km; and improved radiometric accuracy from 7 to 10 bits for LISS-III, and LISS-IV and 10–12 bits for AWiFS. Resourcesat-2 carries two solid-state recorders with a capacity of 200 GB each to store the images taken by its cameras which can be read out later to ground stations. The Resourcesat-2 sensors are shown in Table 2.3, Figs. 2.24, 2.25, 2.26 and 2.27.

2.5.5 China–Brazil Earth Resources Satellite (CBERS) Programme

Initially, the programme included development and deployment of two satellites, CBERS-1 and CBERS-2. Subsequently three additional satellites, CBERS-3, 4 and 4B, have been planned.

Fig. 2.24 Champ elysees as viewed by Quick Bird

Fig. 2.25 Resourcesat-2 LISS-IV image for part of Cuarto, Argentina showing cropland in (in *red* colour and rectangular and circular pattern) and fallow land in different shades of *green* colour. (Arjentina.tif) (Colour Online) *Courtesy* National Remote Sensing Centre, Indian Space Research Organization, Department of Space, Government of India

2.5.5.1 CBERS-1 and -2

The first satellite of the series, CBERS-1, was successfully launched on 14 October, 1999. It is sometimes also called ZY1. It remained functional until August 2003. The second satellite, CBERS-2, was successfully launched on 21 October, 2003. CBERS-1 and -2 are identical satellites. They have three remote sensing multi-spectral cameras:

Wide Field Imager Camera (WFI) This camera records images in two spectral bands: 0.63–0.69 μm (red) and 0.77–0.89 μm (near-infrared), with 260 m spatial resolution and 890 km of ground swath. About 5 days are necessary for a whole coverage of the Earth's surface.

Medium Resolution Camera (CCD) This camera records images in five spectral bands: 0.51–0.73 μm (panchromatic); 0.45–0.52 μm (blue); 0.52–0.59 μm (green);

Fig. 2.26 True colour composite of Skydome, home of the BlueJays, Toronto, Canada as viewed by IKONOS-2

0.63–0.69 μm (red); 0.77– 0.89 μm (near-infrared), with 20 m spatial resolution and 120 km of ground swath. It is possible to operate this camera both on nadir and off-nadir. This last capability allows the system to reduce the temporal resolution from 26 days (nadir operation mode) to 3 days (off-nadir operation mode).

Infrared Multispectral Scanner Camera (IRMSS) This camera records images in four spectral bands: 0.50–1.10 μm (panchromatic); 1.55–1.75 μm (short wave infrared); 2.08–2.35 μm (short wave infrared) and 10.40–12.50 μm (thermal infrared), with 80 m spatial resolution on the three infrared reflected bands and 120 m in the thermal infrared band . Ground swath is 120 km for all the bands of this camera and 26 days are required to obtain a full coverage of the Earth by this camera.

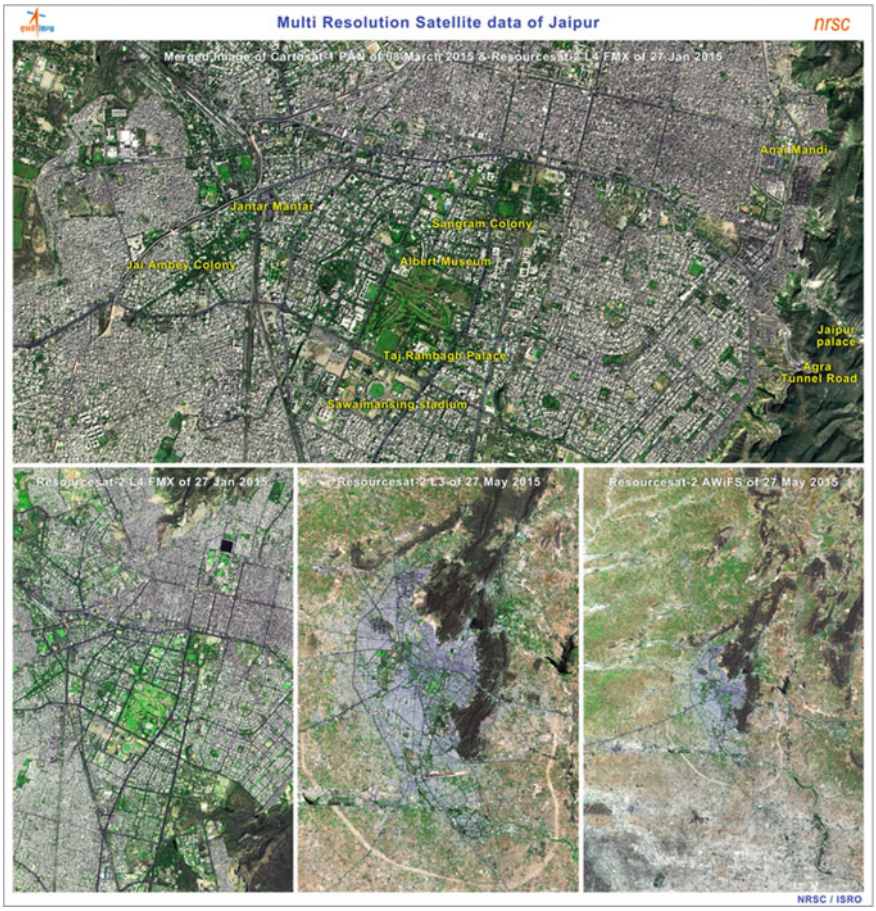

Fig. 2.27 Showing multi-resolution capabilities of IRS series of satellite data. Upper top image shows digitally merged Resourcesat-2 LISS-IV data collected on 8 March, 2015 and Resourcesat-2 LISS-IV satellite image acquired on 27 January, 2015. Lower right image shows Jaipur city, Rajasthan state, India as seen by Resourcesat-2 AWiFS on 27 May, 2015. Lower middle image exhibits Jaipur city as imaged by Resourcesat-2 LISS-III on 27 May, 2015. And the lower left image shows the same city as imaged by Resourcesat-2 LISS-IV on 27 January, 2015. As evident from the figure, as image resolution improves more and more terrain details become clearer (JAIPUR.rar)

2.5.5.2 CBERS-2B

CBERS-2B was launched in 19 September 2007 by a Long-March 4B rocket from the Taiyuan base in China. The satellite operated until June 2010. CBERS-2B is also similar to the two previous members of the series, but a new camera: High-Resolution Panchromatic Camera (HRC) was added to the last satellite: This camera records images in one single panchromatic band 0.50–0.80 μm. The images

recorded by this camera are 27 km width and have 2.7 m spatial resolution. 130 days are required to obtain a full coverage of the Earth by this camera.

2.5.5.3 CBERS-3 and CBERS-4

CBERS-3 was launched in December 2013, but was lost after the Chang Zheng 4B rocket carrying it malfunctioned. The identical CBERS-4 satellite is scheduled for launch during late 2014/mid-2015 (http://en.wikipedia.org/wiki/China%E2%80%93Brazil_Earth_Resources_Satellite_program).

2.5.6 Formosat Satellite Mission

2.5.6.1 Formosat-1

Formosat-1 (Formerly known as Rocsat-1) is an Earth observation satellite operated by the National Space Organization (NSPO) of the Republic of China (Taiwan) to conduct observations of the ionosphere and oceans. It was launched on 27 January, 1999. The payloads aboard Formosat-1 include the Experimental Communication Payload (ECP), Ionosphere Plasma Electrodynamics Instrument (IPEI) and the Ocean Colour Imager (OCI). Formosat-1 is still active as of July 2005. Formosat-2 is a high-resolution optical satellite able to revisit the same point on the globe every day in the same viewing conditions. Its unique orbit and 2 m resolution in panchromatic (0.45–0.90 μm) mode and 8 m in four multispectral bands blue (0.45–0.52 μm), green (0.52–0.60 μm), red (0.63–0.69 μm) and NIR (0.76–0.90 μm) are well suited to change detection and rapid coverage of large areas. With a 20 km swath and cross-track and along-track viewing capability to an extent of ±45° the satellite provides daily coverage of the globe. Orbit of constellation: Circular orbits, altitudes of 800 km, inclinations of 72°; there are six operational planes with 1 satellite per plane, spaced 24° apart.

2.5.6.2 Formosat-2

Formosat-2 was launched on 21 May, 2004 with a high resolution of 2 m panchromatic data and 8 m multispectral satellite image data. The main mission of FORMOSAT-2 is to conduct remote sensing imaging over Taiwan and on terrestrial and oceanic regions of the entire Earth. The images captured by FORMOSAT-2 during daytime can be used for land distribution, natural resources research, forestry, environmental protection, disaster prevention, rescue work and other applications. When the satellite travels to the eclipsed zone, it will observe natural phenomena such as lighting in the upper atmosphere which can be used for

further scientific experiments. FORMOSAT-2 carries both "remote sensing" and "scientific observation" tasks in its mission.

2.5.7 The Earth Observing System Mission

The Terra and Aqua platforms are part of NASA's Earth-observing systems.

2.5.7.1 Terra (EOS-AM)

Terra was launched on 18 December, 1999. With the equatorial crossing time of 10:30 AM of Terra and 1:30 PM for Aqua, they are also known as EOS-AM (Terra) and EOS-PM (Aqua). The principal instruments amongst others on Terra and Aqua are MOderate Resolution Imaging Spectrometer (MODIS) and Advanced Spaceborne Thermal Emission and Reflection Spectrometer (ASTER). Salient features of these sensors are given hereunder:

MOderate Resolution Imaging Spectrometer (MODIS) MODIS is a 36 band spectrometer providing a global dataset every 1–2 days with a 16-day repeat cycle. The spatial resolution of MODIS (pixel size at nadir) is 250 m for channel 1 and 2 (0.6–0.9 μm), 500 m for channel 3–7 (0.4–2.1 μm) and 1000 m for channel 8–36 (0.4–14.4 μm), as in Table 2.4. The MODIS instrument consists of a cross-track scan mirror, collecting optics and individual detector elements. The swath dimensions of MODIS are 2330 km (across track) by 10 km (along-track at nadir). The along track swath dimension is due to the optical setup as well as the scanning mechanism of MODIS. In contrast to other scanning sensors, e.g. AVHRR, MODIS is observing within one scan ten lines of 1 km spatial resolution (40 lines of 250 m resolution and 20 lines of 500 m resolution, respectively) and 12-bit radiometry.

Advanced Spaceborne Thermal Emission and Reflection Radiometer (ASTER) It is the only high spatial resolution instrument aboard Terra, and thus helps bridging the gap between field observations and data from the MODIS and Multi-angle Imaging Spectroradiometer (MISR) instruments, described later. As its name implies, ASTER operates in the visible through thermal infrared portions of the electromagnetic spectrum. Of its 14 bands, three are in the visible and near-infrared (VNIR) between 0.5 and 0.9 μm, six are in the shortwave infrared (SWIR) between 1.6 and 2.43 μm, and five are in the thermal infrared (TIR) between 8 and 12 μm. VNIR channels have 15 m resolution, SWIR have 30 m resolution, and TIR channels have 90 m resolution. ASTER has a 60 km swath width, with a cross-track adjustable swath centre. A special feature of ASTER is an aft pointing additional VNIR telescope for creating stereo views as in Table 2.5. The stereo images have a base-to-height ratio of 0.6. ASTER's repeat cycle is 16 days.

Table 2.4 Specification of the 36 MODIS channels, including primary use, central wavelength, bandwidth and spatial resolution

Primary use	Band number	Central wavelength (nm)	Bandwidth (nm)	Spatial resolution (m)
Land/cloud/aerosols/boundaries	1	645	620–670	250
	2	858.5	841–876	
Land/cloud/aerosols properties	3	469	459–479	500
	4	555	545–565	
	5	1240	1230–1250	
	6	1640	1628–1652	
	7	2130	2105–2155	
Ocean colour/phytoplankton/ biogeochemistry	8	421.5	405–420	1000
	9	443	438–448	
	10	488	483–493	
	11	531	526–536	
	12	551	546–556	
	13	667	662–672	
	14	678	673–683	
	15	748	743–753	
	16	869.5	862–877	
Atmospheric water vapour	17	905	890–920	
	18	936	931–941	
	19	940	915–965	
Surface/cloud temperature	20	3750	3660–3840	
	21	3959	3929–3989	
	22	3959	3929–3989	
	23	4050	4020–4080	
Atmospheric temperature	24	4465.5	4433–4498	
	25	4515.5	4482–4549	
Cirrus clouds/water vapour	26	1375	1360–1390	
	27	6715	6535–6895	
	28	7325	7175–7475	
Cloud properties	29	8550	8400–8700	
Ozone	30	9730	9580–9880	
Surface/cloud temperature	31	11,030	10,780–11,280	
	32	12,020	11,770–12,270	
Cloud top altitude	33	13,335	13,185–13,485	
	34	13,635	13,485–13,785	
	35	13,935	13,785–14,085	
	36	14,235	14,085–14,385	

Table 2.5 Salient features of ASTER sensor

Instrument's parameters	VNIR	SWIR	TIR
Bands	1–3	4–9	10–14
Spatial resolution (m)	15	30	90
Swath width (km)	60	60	60
Cross-track pointing	±318 km (±24°)	±116 km (±8.55°)	±116 km (±8.55°)
Quantization (bits)	8	8	12

Source http://www2.hawaii.edu/~jmaurer/terra/

2.5.7.2 Aqua (EOS PM)

Aqua is a multinational NASA scientific research satellite in orbit around the Earth. It was launched on 4 May, 2002 in a Sun-synchronous polar orbit. Aqua carries six instruments, viz. Advanced Microwave Scanning Radiometer (AMSR-E), MODIS, Advanced Microwave Sounding Unit (AMSU), Atmospheric Infrared Sounder (AIRS), Humidity Sounder for Brazil (HSB), and Clouds and the Earth's Radiant Energy System (CERES) for studies of water on the Earth's surface and in the atmosphere.

Advanced Microwave Scanning Radiometer (AMSR-E)

The Advanced Microwave Scanning Radiometer–Earth-Observing System (AMSR-E) is a twelve-channel, six-frequency, passive microwave radiometer system. It measures horizontally and vertically polarized brightness temperatures at 6.9, 10.7, 18.7, 23.8, 36.5 and 89.0 GHz. Spatial resolution of the individual measurements varies from 5.4 km at 89 GHz to 56 km at 6.9 GHz. AMSR-E uses an offset parabolic reflector, 1.6 m in diameter, to focus Earth-emitted microwave radiation into an array of six feedhorns, which then feed the radiation to the detectors. It measures cloud properties, sea surface temperature, near-surface wind speed, radiative energy flux, surface water, ice and snow. The AMSR-E data have been found quite useful in studying the regional-level soil moisture status (http://nsidc.org/data/docs/daac/amsre_instrument.gd.html) (Accessed on 30 November 2014).

Moderate Resolution Imaging Spectroradiometer (MODIS)

The MODIS aboard Aqua mission is similar to the one that is aboard Terra satellite. Since Terra passes over equator in the forenoon (around 10:30 Hrs) and Aqua in the afternoon around 14:30 Hrs they provide daily two coverages on an area of interest that is very useful in studying the dynamic phenomenon (http://www2.hawaii.edu/~jmaurer/terra/).

Multi-angle Imaging Spectroradiometer (MISR)

The MISR instrument measures the Earth's brightness in four spectral bands, at each of nine look angles spread out in the forward and aft directions along the flight line. Spatial samples are acquired every 275 m. Over a period of 7 min, a 360 km wide

swath of Earth comes into view at all nine angles. Each MISR camera sees instantaneously a single row of pixels at right angles to the ground track in a push broom format. It records data in four bands: blue, green, red and near-infrared. Each camera has four independent linear CCD arrays (one per filter), with 1504 active pixels per linear array (http://eo1.usgs.gov/). MISR provides new types of information for scientists studying Earth's climate, such as the partitioning of energy and carbon between the land surface and the atmosphere, and the regional and global impacts of different types of atmospheric particles and clouds on climate. The change in reflection at different view angles affords the means to distinguish different types of atmospheric particles (aerosols), cloud forms and land surface covers. Combined with stereoscopic techniques, this enables construction of 3-D models and estimation of the total amount of sunlight reflected by Earth's diverse environments https://www-misr.jpl.nasa.gov/Mission/ (Accessed on 30 November 2014).

2.5.8 *Earth Observing-1 (EO-1) Mission*

As a test bed for proving newer and challenging sensor technologies, the EO-1 satellite was launched on 21 November, 2000. EO-1 sensor Hyperion is a hyper spectral sensor which offers data in 220 spectral bands 16 km swath and 30 m spatial resolution. EO-1/Hyperion offer the highest available spectral resolution in the field of satellite-borne remote sensing systems. The satellite carries three sensors, namely hyperion, advanced land imager (ALI) and atmospheric corrector (AC) as in Table 2.6.

The Hyperion provides a high-resolution hyperspectral imager capable of resolving 220 spectral bands (0.4–2.5 μm) with a 30 m resolution. The instrument can image a 7.5 km by 100 km land area per image and provide detailed spectral mapping across all 220 channels with high radiometric accuracy. The Hyperion is a push broom instrument. Each image frame taken in push broom configuration images the spectrum of a line 302 m long by 7.5 km wide (perpendicular to the satellite motion). Frames are then combined to form a two-dimensional spatial image with a complete spectral signature for each pixel. Hyperion has a single telescope and two spectrometers, one visible/near-infrared (VNIR380 to 1000 nm)

Table 2.6 Salient features of EO-1 sensors

Parameters	EO-1		
	ALI	Hyperion	AC
Spectral range	0.4–2.4	0.4–2.4	0.9–1.6
Spatial resolution (m)	30	30	250
Swath width (km)	36	7.6	185
Spectral resolution	Variable	10 nm	6 nm
Spectral coverage	Discrete	Continuous	Continuous
Pan band resolution	10 m	N/A	N/A
Total number of bands	10	220	256

spectrometer and one short wave infrared (SWIR-900 to 2500 nm) spectrometer. The Hyperion sensor on-board the EO-1 satellite is the first hyperspectral sensor to operate from space.

Advanced Land Imager (ALI) The Advanced Land Imager (ALI) is the first Earth-observing instrument to be flown under NASA's New Millennium Programme (NMP). The ALI employs novel wide-angle optics and a highly integrated multispectral and panchromatic spectrometer. Operating in a push broom fashion at an orbit of 705 km, the ALI provides Landsat-type panchromatic and multispectral bands. These bands have been designed to mimic six Landsat bands with three additional bands covering 0.433–0.453, 0.845–0.890 and 1.20–1.30 μm. The ALI also contains wide-angle optics designed to provide a continuous 15° × 1.625° field of view for a fully populated focal plane with 30 m resolution for the multispectral pixels and 10 m resolution for the panchromatic pixels.

Atmospheric Corrector The images of the Earth acquired by satellites are degraded by atmospheric absorption and scattering. The spectral measurements made by the LEISA (Linear Etalon Imaging Spectral Array) *Atmospheric Corrector* (LAC or AC) enable improving the accuracy of surface reflectance estimates. It provides the following capabilities via a compact and simple bolt-on design for future Earth Science, land imaging missions: The EO-1 Advanced Land Imager salient features as shown in Tables 2.7 and 2.8.

- High spectral, moderate spatial resolution hyperspectral imager using a wedge filter technology.
- Spectral coverage of 0.85–1.5 um; bands are selected for optimal correction of high spatial resolution images.
- Correction of surface imagery for atmospheric variability (primarily water vapour) http://eo1.usgs.gov/sensors/leisa (Accessed on 30 November 2014).

Table 2.7 Salient features of EO-1 advanced land imager

Band	Wavelength (μm)		Ground sample distance (m)	
Pan	0.48–0.69			10
MS-1	0.433–0.453	30		
MS-1′	0.045–0.515			30
MS-2	0.525–0.605	30		
MS-3	0.63–0.69			30
MS-4	0.775–0.805	30		
MS-4′	0.845–0.89			30
MS-5′	1.2–1.3		30	
MS-5	1.55–1.75	30		
MS-7	2.08–2.35	30		

Source http://eo1.usgs.gov/sensors/ali Accessed on 30 November 2014

2.5.9 RapidEye

The RapidEye satellite constellation is a dedicated system for commercial Earth observation, consisting of five mini-satellites, which carry a CCD-based imaging system. The CCD-based Earth imaging system (6 spectral bands including visible, near infrared and panchromatic) will consist of two cameras allowing the generation of images of up to 150 km × 1000 km at a resolution of 6.5 m. The RapidEye Mission was launched in 2008 (Table 2.8) Anonymous 2016. Rapid Eye imagery product specifications. Version 6.3 January 2016. The five satellites were launched on one vehicle and placed in a common Sun-synchronous orbit of 620 km, with the satellites equally spaced about 19 min apart in their orbit, ensuring frequent imaging of particular areas of interest. The satellites can be redirected anytime through the telemetry, tracking and command unit. A data handling and storage unit is situated on board each satellite as well as a high-speed X-band communication system. The designed lifetime of these satellites is 7 years. Each satellite has the capability of performing an off-track rotation. The camera's imaging swath of approx. 150 km combined with an off-track angle of ±22° ensures daily global accessibility. On 6 November 2013 RapidEye officially changed its name to BlackBridge (http://blackbridge.com/rapideye/news/pr/2013-blackbridge.htm http://space.skyrocket.de/doc_sdat/rapideye-1.htm30-11-2014).

Table 2.8 RapidEye satellite sensor specifications

Number of satellites	5
Orbit altitude	630 km in sun-synchronous orbit
Equator crossing time	11:00 am local time (approximately)
Sensor type	Multi spectral push broom imager
Spectral bands	Wavelength (nm)
	440–510
	520–590
	630–685
	690–730
	760–850
Ground sampling distance (nadir)	6.5 m
Pixel size (orthorectified)	5 m
Swath width	77 km
On-board data storage	1500 km of image data per orbit
Revisit time	Daily (off-nadir)/5.5 days (at nadir
Dynamic range	12 bit

Source http://www.satimagingcorp.com/satellite-sensors/other-satellite-sensors/rapideye/ Accessed on 30 November 2014

2.5.10 High Spatial Resolution Remote Sensing Systems

Consequent upon a decision of the United States government made in 1994 to allow civil commercial companies to market high spatial resolution remote sensor data (approximately 1 × 1 to 4 × 4 m), several commercial consortiums, namely Space Imaging Inc., ORBIMAGE, Inc., Earth Watch, Inc. have launched satellites providing high spatial resolution data to the user community across the world.

2.5.10.1 Earlybird and QuickBird

EarlyBird was launched in 1996 with a 3 m panchromatic band and three visible to near-infrared (VNIR) bands at 15 m spatial resolution. Unfortunately, Earth Watch, subsequently lost contact with the satellite. QuickBird was launched on 18 October, 2001. Interestingly, it is in a 66° non-sun-synchronous orbit. Revisit times range from 1 to 5 days, depending on latitude. It has a swath width of 20–40 km. QuickBird has 0.61 m (at nadir) panchromatic band (445–900 nm) and four visible/near-infrared bands at 2.4 m (at nadir) spatial resolution. The data are quantized to 11 bits (brightness values from 0 to 2047). The sensor may be pointed fore and aft and across track to obtain stereoscopic data (Fig. 2.28).

2.5.10.2 Ikonos

Space imaging, Inc., launched IKONOS on 27 April 1999. Unfortunately, contact was lost with the satellite 8 min after launch. Space Imaging Inc. successfully launched a second IKONS on 24 September 1999. The IKONS has a 1 m panchromatic band and four multispectral visible and near-infrared bands at 4 m spatial resolution . It has both cross-track and along-track viewing instruments, which enables flexible data acquisition and frequent revisit capability : <3 days at 1 m spatial resolution (for look angles <26°) and 1.5 days at 4 m spatial resolution. The nominal swath width is 11 km. Data are quantized to 11 bits (Fig. 2.29).

2.5.10.3 Orbview-3

Launched by GeoEye on 26 June, 2003, OrbView-3 had a panchromatic band with 1 m spatial resolution and four visible and near-infrared multispectral bands at 4 m spatial resolution and 8 km swath. The sensor's repetivity on Earth was less than 3 days, with an ability to turn side to side 45°. On 23 April, 2007, GeoEye announced that the OrbView-3 mission was terminated.

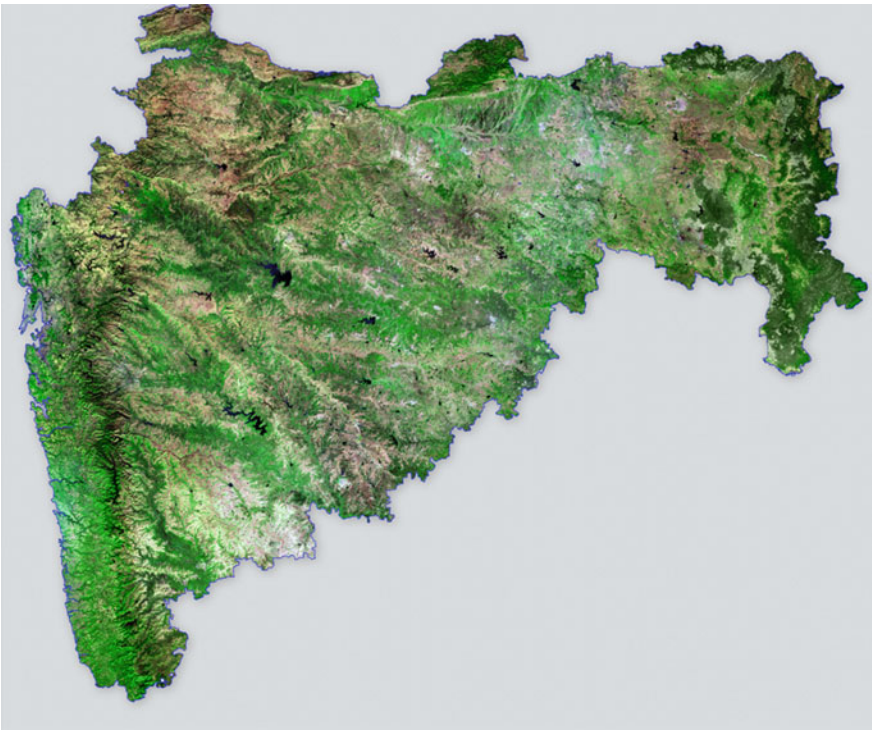

Fig. 2.28 Natural colour composite resourcesat-2 LISS-III image mosaic of Maharashtra state, central-western India (*green* colour indicates different types of vegetation) (Maha_mosaic.tif) (*Courtesy* National Remote Sensing Centre, Indian Space Research Organization, Department of Space, Government of India)

2.5.10.4 Cartosat Mission

The Cartosat mission aimed at designing and developing an advanced 3-axis body stabilized remote sensing satellite for providing enhanced spatial resolution with stereo imaging capability for cartographic applications.

Cartosat-1 was launched by the Indian Space research organization (ISRO) on 5 May, 2005. Cartosat-1 carries two panchromatic cameras that take black-and-white stereoscopic images in the visible region of the electromagnetic spectrum as in Fig. 2.30. The satellite images have a spatial resolution of 2.5 m and cover a swath of 30 km. The cameras are mounted on the satellite in such a way that near simultaneous imaging of the same area from two different angles is possible. This facilitates the generation of accurate three-dimensional maps. The cameras manoeuver across the direction of the satellite's movement to facilitate the imaging of an area more frequently. Cartosat-1 also carries a Solid State Recorder with a capacity of 120 GB to store the images taken by its cameras. The stored images can be transmitted when the satellite comes within the visibility zone of a ground station.

Fig. 2.29 Resourcesat-1 AWiFS image mosaic covering India and its environ (India_mosaic.tif) (*Courtesy* National Remote Sensing Centre, Indian Space Research Organization, Department of Space, Government of India)

Cartosat-2 is an advanced remote sensing satellite capable of providing scene-specific spot imagery. The panchromatic camera (PAN) on-board the satellite can provide imagery with a spatial resolution of better than 1 m and a swath of 9.6 km. The satellite can be steered up to 45° along as well as across the track. Satellite has been placed in Sun-synchronous polar orbit at an altitude of 630 km. It has a revisit period of 4 days which can be improved to 1 day with suitable orbit manoeuver (Fig. 2.31).

Fig. 2.30 Perth airport, Australia as seen by Cartosat-2 (Courtesy: National Remote Sensing Centre, Indian Space Research Organization, Department of Space, Government of India)

Cartosat-2A is the thirteenth satellite in the Indian Remote Sensing Satellite series (IRS). It is a sophisticated and rugged remote sensing satellite that can provide scene-specific spot imagery. The satellite carries a Panchromatic camera (PAN). The spatial resolution of this camera is better than 1 m and swath of 9.6 km.

Cartosat-2B Launched on 12 July, 2010, Cartosat-2B carries a panchromatic camera (PAN) similar to those of its predecessors—Cartosat-2 and -2A. It is capable of imaging a swath (geographical strip) of 9.6 km with a resolution of better than 1 m. The highly agile Cartosat-2B is steerable up to ±26° along as well as across track to obtain stereoscopic imagery and achieve a 4- to 5-day revisit capability. The scene-specific spot imagery sent by Cartosat-2B's PAN is useful for cartographic and a host of other applications http://www.isro.org/satellites/cartosat-2b.aspxAccessed on 30 November 2014

2.5.10.5 GeoEye-1

The GeoEye-1 was launched on 6 September 2008 and is capable of acquiring image data at 0.41 m panchromatic (B&W) and 1.65 m multispectral resolution. It also features a revisit time of less than 3 days, as well as the ability to locate an object within just three metres of its physical location. Sample images of cartosat-2 are appended as Figs. 2.32 and 2.33.

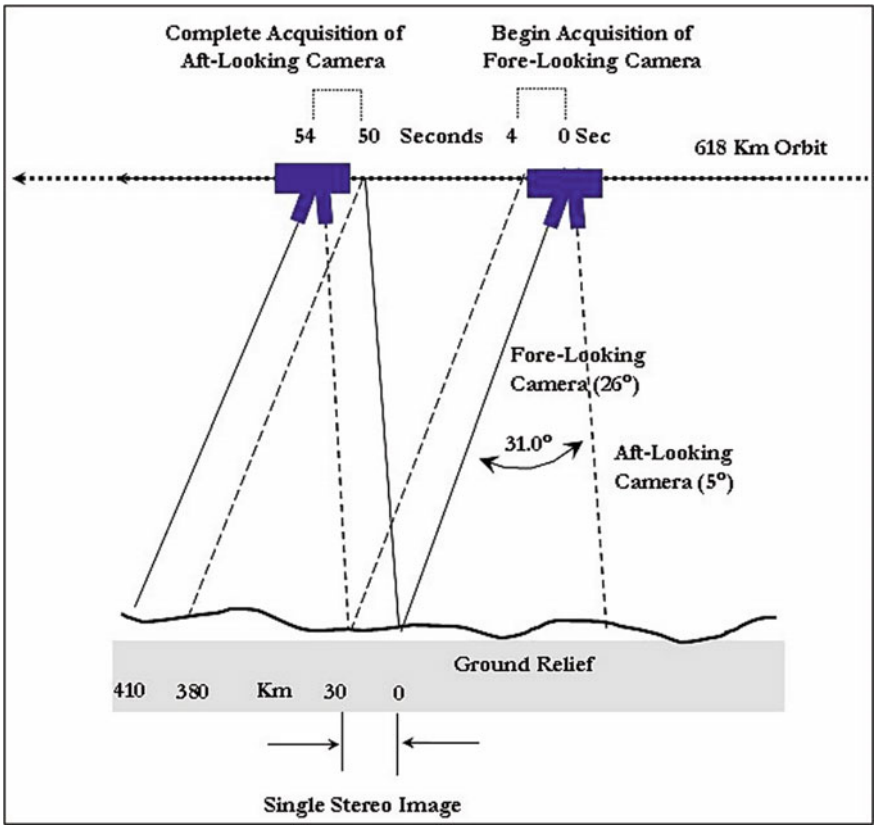

Fig. 2.31 Cartosat-1 stereo imaging (*Courtesy* National Remote Sensing Centre, Indian Space Research Organization, Department of Space, Government of India)

2.5.10.6 WorldView Missions

WorldView-1 Launched on 18 September 2007, WorldView-1 is operating at an altitude of 496 km. It has an average revisit time of 1.7 days and captures panchromatic images of 17.6 km wide strip of the Earth with 0.50 m spatial resolution and 11-bit radiometry. The satellite is also equipped with state-of-the-art geolocation capabilities and exhibits stunning agility with rapid targeting and efficient in-track stereo collection. Source: http://www.satimagingcorp.com/satellite-sensors/worldview-2/.

WorldView-2 Launched on 8 October 2009, WorldView-2 satellite provides 0.46 m panchromatic (B&W) mono- and stereo satellite image data. With its improved agility, it is able to act like a paintbrush, sweeping back and forth to collect very large areas of multispectral imagery in a single pass. And the combination of WorldView-2s increased agility and high altitude enables it to typically revisit any place on Earth in 1.1 days. When added to the satellite constellation,

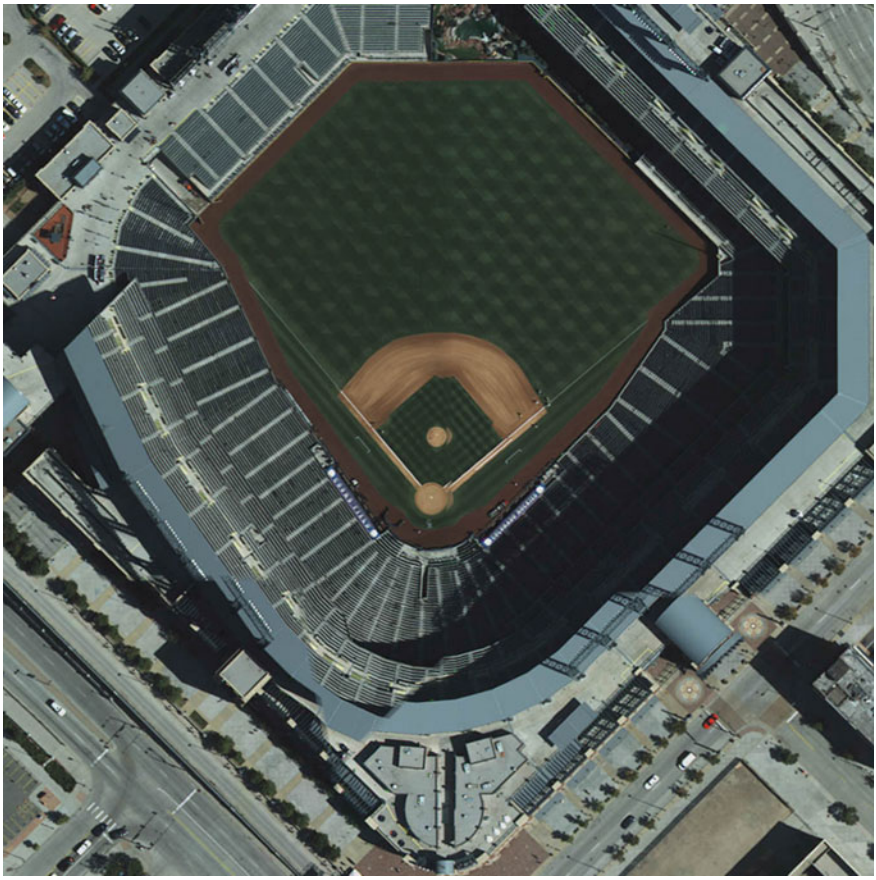

Fig. 2.32 Coors field Denver as viewed by GeoEye

revisit time drops below 1 day and never exceeds 2 days, providing the most same-day passes of any commercial high-resolution constellation. The WorldView-2 sensor provides a high-resolution Panchromatic band and eight (8) multispectral bands; four (4) standard colours (red, green, blue and near-infrared 1) and four new bands, namely coastal (400–450 nm); yellow (585–625 nm), red edge (705–745 nm), and near-infrared (860–1040 nm) for various applications.

WorldView-3 WorldView-3 was launched on 13 August 2014 at an altitude of 617 km. It provides 31 cm panchromatic resolution, 1.24 m multispectral resolution and 3.7 m shortwave infrared resolution. It has an average revisit time of less than 1 day as in Table 2.9.

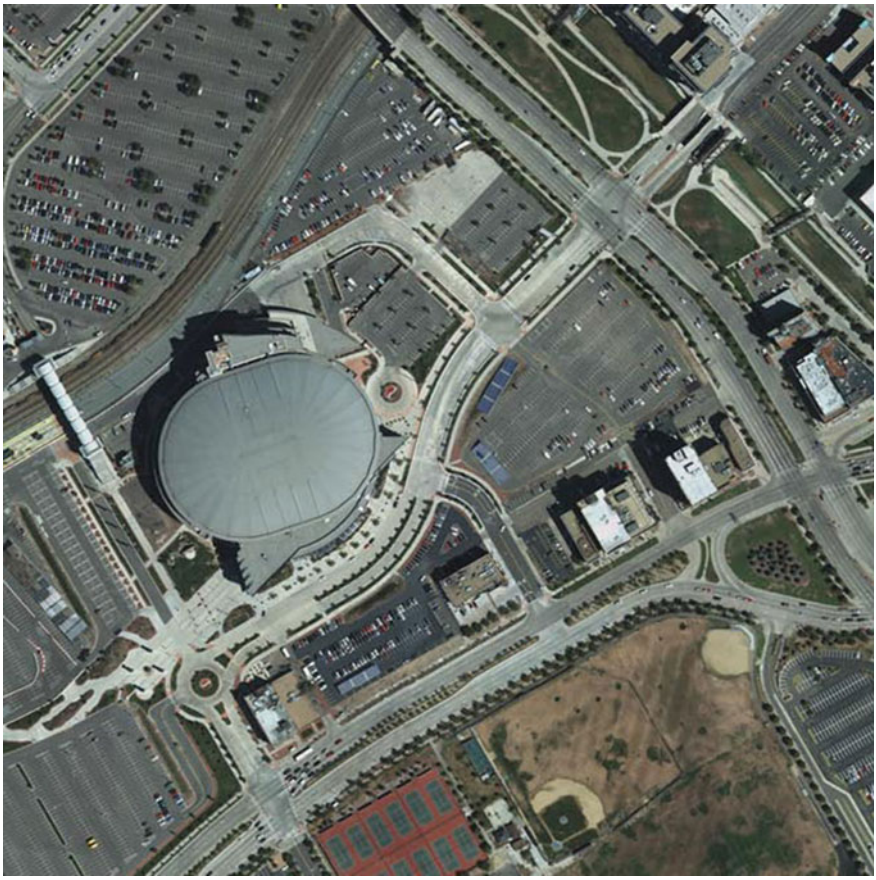

Fig. 2.33 Pepsi centre Denver, Toronto as viewed by GeoEye

2.6 The NOAA Missions

Complementing the geostationary satellites are two polar-orbiting satellites known as Advanced Television Infrared Observation Satellite (TIROS-N or ATN), constantly circling the Earth in an almost north–south orbit, passing close to both poles. The orbits are circular, with an altitude between 830 (morning orbit) and 870 (afternoon orbit) km, and are Sun synchronous. One satellite crosses the equator at 7:30 a.m. local time, the other at 1:40 p.m. local time. The circular orbit permits uniform data acquisition by the satellite and efficient control of the satellite. Operating as pair, these satellites ensure that data for any region of the Earth are no more than six hours old.

The primary instrument aboard the satellite is the Advanced Very High Resolution Radiometer (AVHRR). This scanning radiometer uses six detectors that

Table 2.9 Salient features of WorldView-3 mission

Orbit	Altitude:617 km Type: Sun sync, 1:30 pm descending node Period: 97 min
Sensor bands	Panchromatic: 450–800 nm 8 Multispectral: (red, red edge, coastal, blue, green, yellow, near-IR1 and near-IR2) 400–1040 nm, 8SWIR: 1195–2365 nm 12 CAVIS Bands: (desert clouds, aerosol-1, aerosol-2, aerosol-3, green, water-1, water-2, water-3, NDVI-SWIR, cirrus, snow) 405–2245 nm
Sensor resolution (or GSD, ground sample distance; off-nadir is geometric mean)	Panchromatic nadir: 0.31 m GSD at Nadir 0.34 m at 20° Off-Nadir Multispectral nadir: 1.24 m at Nadir, 1.38 m At 20° Off-Nadir SWIR Nadir: 3.70 m at Nadir, 4.10 m At 20° Off-Nadir CAVIS Nadir: 30.00 m
Dynamic range	11-bits per pixel Pan and MS; 14-bits per pixel SWIR
Swath width	At nadir: 13.1 km
On-board storage	2199 Gb solid state with EDAC
Revisit frequency(at 40° N Latitude)	1 m GSD: <1.0 day 4.5 days at 20° off-nadir or less
Geolocation accuracy (CE90)	Predicted performance: <3.5 m CE90 without ground control

Source http://www.satimagingcorp.com/satellite-sensors/worldview-3/

collect different bands of radiation wavelengths (Table 2.10). The first AVHRR was a 4-channel radiometer, first carried on TIROS-N (launched October 1978). This was subsequently improved to a 5-channel instrument (AVHRR/2) that was initially carried on NOAA-7 (launched June 1981). The latest instrument version is AVHRR/3, with six channels, first carried on NOAA-15 launched in May 1998.

Measuring the same view, this array of diverse wavelengths, after processing, permits multi-spectral analysis for more precisely defining hydrologic, oceanographic and meteorological parameters (http://noaasis.noaa.gov/NOAASIS/ml/avhrr.html) accessed on 30 November 2014.

NOAA-19 is operational now. It will be replaced by Joint Polar Satellite, System (JPSS-1/NOAA-20) in early 2017. JPSS-1/NOAA-20 will have the following sensors: (1) VIIRS, (2) CrIS, (3) ATMS, (4) OMPS-N and (5) CERES-FM6. It is the second spacecraft within NOAA's next generation of polar-orbiting satellites. It is scheduled to launch in early 2017. VIIRS is a scanning radiometer that collects imagery and radiometric measurements of the land, atmosphere, cryosphere and oceans in the visible and infrared bands of the electromagnetic spectrum. JPSS-1 will be followed by JPSS-2 in 2021, JPSS-3 in 2026 and JPSS-4 in 2031, respectively.

Table 2.10 AVHRR/3 channel characteristics

AVHRR/3 channel characteristics			
Channel number	Resolution at nadir (km)	Wavelength (μm)	Typical use
1	1.09	0.58–0.68	Daytime cloud and surface mapping
2	1.09	0.725–1.00	Land–water boundaries
3A	1.09	1.58–1.64	Snow and ice detection
3B	1.09	3.55–3.93	Night cloud mapping, sea surface temperature
4	1.09	10.30–11.30	Night cloud mapping, sea surface temperature
5	1.09	11.50–12.50	Sea surface temperature

2.6.1 JPSS Satellites

The JPSS represents the second generation of U.S operational polar-orbiting satellites. The programme envisages the launch of three satellites: the Suomi National Polar-orbiting Partnership (SNPP), JSPP-1 and JSPP-2. The SNPP (Often referred to as Suomi NPP) was launched October 2011; the JPSS-1 has a planned launch date of 2017 and the anticipated launch date for JPSS-2 IS 2022. Visible Infrared Imaging Radiometer Suite (VIIRS) VIIRS, a scanning radiometer, collects visible and infrared imagery and radiometric measurements of the land, atmosphere, cryosphere and oceans. VIIRS data are used to measure cloud and aerosol properties, ocean colour, sea and land surface temperature, ice motion and temperature, fires, and Earth's albedo.

2.7 Spaceborne Imaging Microwave Systems

Salient features of various satellites carrying microwave radar systems are discussed hereafter.

2.7.1 Seasat

Launched in 1978, Seasat was the first civilian remote sensing satellite to carry a spaceborne synthetic aperture radar (SAR) sensor. The SAR is operated at L-band (23.5 cm) with HH polarization. The viewing geometry was fixed between 9° and 15° with a swath width of 100 km and a spatial resolution of 25 m. This steep viewing geometry was designed primarily for observations of ocean and sea ice. However, a great deal of images was also collected over land areas.

2.7.2 European Remote Sensing Satellite (ERS-1 and -2)

The European Space Agency (ESA) had launched ERS-1 in July 1991. ERS-1 carried on-board a radar altimeter, an infrared radiometer and microwave sounder, and a C-band (5.66 cm) active microwave instrument. This is a flexible instrument which could be operated as a scatter metre to measure reflectivity of the ocean surface, as well as ocean surface wind speed and direction. It can also operate as synthetic aperture radar (SAR), collecting imagery over a 100 km swath over an incidence angle range of 20°–26°, at a resolution of approximately 30 meters with VV polarization. Generally, the repeat cycle is about 35 days. ERS-1 failed on 10 March 2000, far exceeding its expected lifespan.

ERS-2, the successor of ERS-1, was launched on 21 April 1995. Largely identical to ERS-1, it added additional instruments, namely GOME (Global Ozone Monitoring Experiment)—a nadir scanning ultraviolet and visible spectrometer, and ATSR-2 included three visible spectrum bands specialized for chlorophyll and vegetation. Besides, improvements to existing instruments were made. When ERS-2 was launched, ERS-1 shared the same orbital plane. This allowed a tandem mission, with ERS-2 passing the same point on the ground 1 day later than ERS-1 which has enabled making interferometric observations (repeat-pass interferometry). ERS-2 has a repeat cycle of 35 days. ERS-2 has been operating without gyroscopes since February 2001, resulting in some degradation of the data provided by the instruments.

The successor to ERS-2 is Envisat containing improved versions of many of the instruments on-board ERS-2; however, its operational life was increased until 2011. Over a series of burns in July, August and September, ERS-2 was finally depleted of all fuel on 5 September 2011. ESA is developing five new missions called Sentinels specifically for the operational needs of the Copernicus programme.

2.7.3 Sentinel-1

Sentinel-1 is a two-satellite constellation with the prime objectives of land and ocean monitoring. The goal of the mission is to provide C-Band SAR data continuity following the retirement of ERS-2 and the end of the Envisat mission. The first Sentinel-1A satellite with C-band SAR was launched on 3 April 2014. The C-band SAR aboard Sentinel-1A collects the data in the following four modes: (i) Strip map mode: 80 km swath, 5 × 5 m spatial resolution; (ii) Interferometric wide swath: 250 km swath, 5 × 20 m spatial resolution; (iii) Extra-wide swath mode: 400 km Swath, 25 × 100 m spatial resolution; and (iv) Wave-mode: 20 km × 20 km, 5 × 20 m spatial resolution (http://en.wikipedia.org/wiki/Sentinel-1).

2.7.4 Japanese Earth Resources Satellite (JERS-1)

Launched by the National Space Development Agency of Japan (NASDA) in February 1992, the JERS-1 carries a L-Band (23.5 cm) SAR operating at HH polarization in addition to two optical sensors. The swath width is approximately 75 km and spatial resolution is approximately 18 m in both range and azimuth. The imaging geometry of JERS-1 is slightly shallower than either SEASAT or the ERS satellites, with the incidence angle at the middle of the swath being 35°. Thus, JERS-1 images are slightly less susceptible to geometry and terrain effects. The longer L-band wavelength of JERS-1 allows some penetration of the radar energy through vegetation and other surface types.

2.7.5 Advanced Land Observation Satellite (ALOS-1)

Land Observation Satellite (ALOS) was launched on 24 January 2006. The ALOS (renamed "Daichi") has three remote sensing instruments: the Panchromatic Remote-sensing Instrument for Stereo Mapping (PRISM) for digital elevation mapping (DEMs), the Advanced Visible and Near Infrared Radiometer type 2 (AVNIR-2) for precise land cover observation and the Phased Array type L-band Synthetic Aperture Radar (PALSAR) for day-and-night and all-weather land observation and enables precise land cover observation and can collect enough data by itself for mapping on a scale of 1:25,000, without relying on points of reference on the ground. The Advanced Visible and Near Infrared Radiometer type 2 (AVNIR-2) operates in four spectral bands, viz. blue (0.42–0.50 μm), green (0.52–0.60 μm), red (0.61–0.69 μm) and near-IR (0.76–0.89 μm) with 10 m spatial resolution. The PRISAM provides stereoscopic panchromatic (0.52–0.77 μm) images of the Earth at 2.5 m spatial resolution. The PALSAR (L-band SAR), another sensor, images the Earth at 10 and 100 m spatial resolution. The mission was operational till 12 May 2011. A sample image captured by ALOS-PALSAR is appended as shown in Fig. 2.34.

ALOS-2

The Advanced Land Observing Satellite-2 (ALOS-2), a follow-on mission of ALOS-1 was launched on 24 May 2014. The PALSAR-2 aboard ALOS-2 is an L-band Synthetic Aperture Radar (SAR) sensor, a microwave sensor that emits L-band radio waves and receives their reflection from the ground to acquire information.

The PALSAR-2 has three modes:

Spotlight mode: The most detailed observation mode with 1 by 3 m resolution (observation width of 25 km).

Strip Map mode: A high-resolution mode with the choice of 3, 6 or 10 m resolution (observation width of 50 or 70 km).

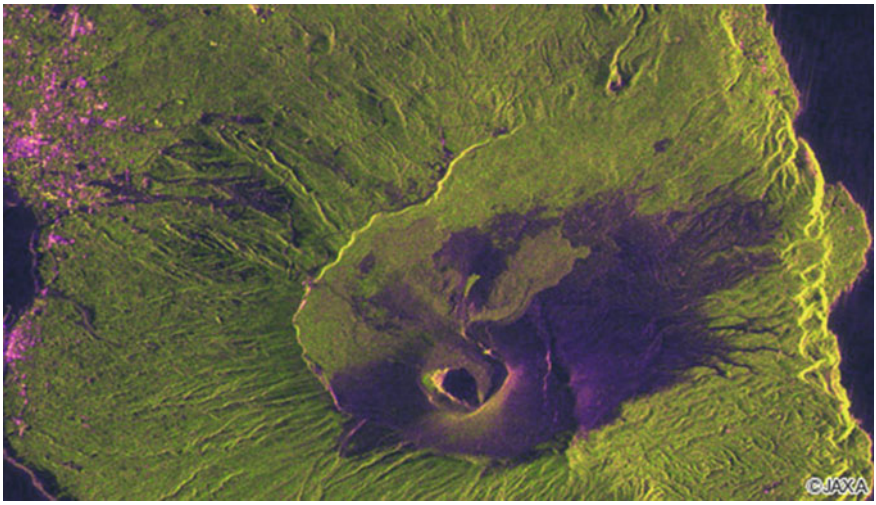

Fig. 2.34 Izuoshima, an uninhabited volcanic island in Japan as viewed by ALOS-PALSAR

ScanSAR mode: A broad area observation mode with observation width of 350 or 490 km, and resolution of 100 or 60 m, respectively.

The imaging modes of ALOS-2 are shown in Fig. 2.35. It has only microwave sensor (PALSAR-2) operating in 1.2 GHz (L-band) with several operational mode. In spotlight mode the spatial resolution is 1–3 m (Table 2.11) (http://www.eorc.jaxa.jp/ALOS/en/about/palsar.htm).

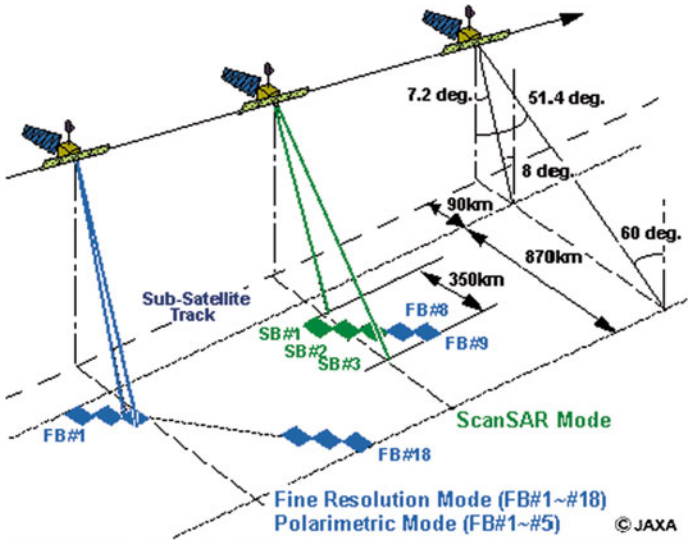

Fig. 2.35 The imaging modes of ALOS-2 mission (http://www.eorc.jaxa.jp/ALOS/en/about/palsar.htm)

Table 2.11 PALSAR-2 specifications

Observation mode	Stripmap[a]			Full (Quad.) polarimetry[a]	
	(3 m)	(6 m)	(10 m)	(6 m)	(10 m)
Obs. Mode ID (code)	UBS/UBD	HBS/HSD	FBS/FBD	HBQ	FBQ
Width (East–West) (Length of range direction)	55 km (max)	55 km (max)	70 km (max)	40-50 km	30 km
Length (North–South) (Length of azimuth direction)	70 km	70 km	70 km	70 km	70 km
Time duration of azimuth direction	10 sec	10 sec	10 sec	10 sec	10 sec
Range resolution*1	3.0 m	6.0 m	9.1 m	5.1 m	8.7 m
Azimuth resolution*1	3.0 m	4.3 m	5.3 m	4.3 m	5.3 m
Pixel spacing levels 1.5/3.1	2.5 m	3.125 m	6.25 m (2look)	3.125 m	6.25 m (2look)
Pixel spacing level 2.1	2.5 m/5.0 m/10.0 m	3.125 m/6.25 m/12.5 m	6.25 m/12.5 m	3.125 m/6.25 m/12.5 m	6.25 m/12.5 m
Polarization	Single (HH, HV, VH, or VV) Dual (HH + HV or VH + VV)			Full (Quad.) polarimetry (HH + HV + VH + VV)	

[a]Stripmap and Full (Quad.) polarimetry modes define category names by resolution: Ultra-Fine(3 m), High-sensitive (6 m), Fine (10 m) http://en.alos-pasco.com/alos-2/palsar-2/ accessed on 26-07-2016

2.7.6 Radarsat Missions

2.7.6.1 Radarsat-1

Launched on 4 November 1995, Radarsat-1 provided Canada and the world with an operational radar satellite system capable of timely delivery of large amounts of data. With 24-day repeat cycle Radarsat-1 acquired images of the Earth in the beam modes given in Table 2.13 and Fig. 2.36. Radarsat-1 carries an advanced C-band (5.6 cm), HH-polarized SAR with a steerable radar beam allowing various imaging options over a 500 km range. Imaging swaths can be varied from 35 to 500 km in width, with resolutions from 10 to 100 m. Viewing geometry is also flexible, with incidence angles ranging from less than 20° to more than 50°. Although the satellite's orbit repeat cycle is 24 days, the flexibility of the steerable radar beam gives Radarsat the ability to image regions much more frequently and to address specific geographic requests for data acquisition. Radarsat's orbit is optimized for frequent coverage of mid-latitude to Polar regions, and is able to provide daily images of the entire Arctic region as well as view any part of Canada within 3 days. Even at equatorial latitudes, complete coverage can be obtained within 6 days using the widest swath of 500 km.

2.7.6.2 Radarsat-2

Radarsat-2 was launched on 14 December 2007. It has a Synthetic Aperture Radar (SAR) with multiple polarization modes. Its highest spatial resolution is 3 m with 100 m positional accuracy. The repeat cycle of Radarsat-2 is 24 days. Radarsat-2 is follow on to Radarsat-1. It has the same orbit (798 km altitude Sun-synchronous

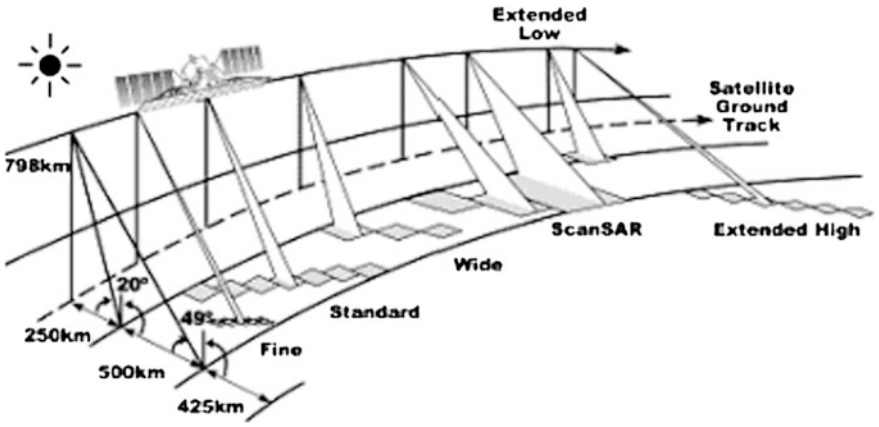

Fig. 2.36 Image acquisition modes of Radarsat1SAR (*Credit*: *Canadian Space Agency*) (http://imaging.geocomm.com/features/sensor/radarsat1/) (Accessed on 21 July 2016)

with 6 p.m. ascending node and 6 a.m. descending node). Radarsat-2 salient features of different beam modes as in Table 2.12 are separated by half an orbit period (~50 min) from Radarsat-1 (in terms of ground track it would represent ~12 days ground track separation). It is intended to fill a wide variety of roles, including sea ice mapping and ship routing, iceberg detection, agricultural crop monitoring, marine surveillance for ship and pollution detection, terrestrial defense surveillance and target identification, geological mapping, land use mapping, wetlands mapping, soil moisture estimation, and topographic mapping.

2.7.6.3 RADARSAT Constellation Mission (RCM)

The successor (and complementary) mission to RADARSAT-2 will be consisting of three (small) spacecrafts (with a potential to increase the number to six). RCM is an evolution of the RADARSAT programme with improved operational use of SAR data and improved system reliability. The overall objective of RCM is to provide C-band SAR data continuity for the RADARSAT-2 users, as well as adding a new series of applications enabled through the constellation approach (Fig. 2.37). Operating in C-band (5.405 GHz) with 100 MHz bandwidth SAR on-board RCM will image the Earth at HH, VV and HV. HV and compact polarimetry will provide 1 × 3 m spatial resolution in spotlight mode (Fig. 2.38) (http://www.asc-csa.gc.ca/eng/satellites/radarsat/radarsat-tableau.asp).

2.7.7 Envisat

Environmental SATellite (ENVISAT) was launched into a Sun-synchronous polar orbit at an altitude of 790 km (490 mi) [±10 km (6.2 mi)] on 1 March 2002 aboard. It orbits the Earth in about 101 min with a repeat cycle of 35 days. After losing contact with the satellite on 8 April 2012, ESA formally announced the end of Envisat's mission on 9 May 2012. Envisat carried an array of nine Earth observation instruments that gathered information about the Earth (land, water, ice

Table 2.12 Image acquisition modes of Radarsat-1 SAR instrument

Beam modes	Nominal Swath Width (km)	Nominal resolution (m)
Fine resolution	45	8
Standard	100	30
Wide	150	30
ScanSAR narrow	300	50
ScanSAR wide	500	100
Extended high incidence	75	18–27
Extended low incidence	170	30

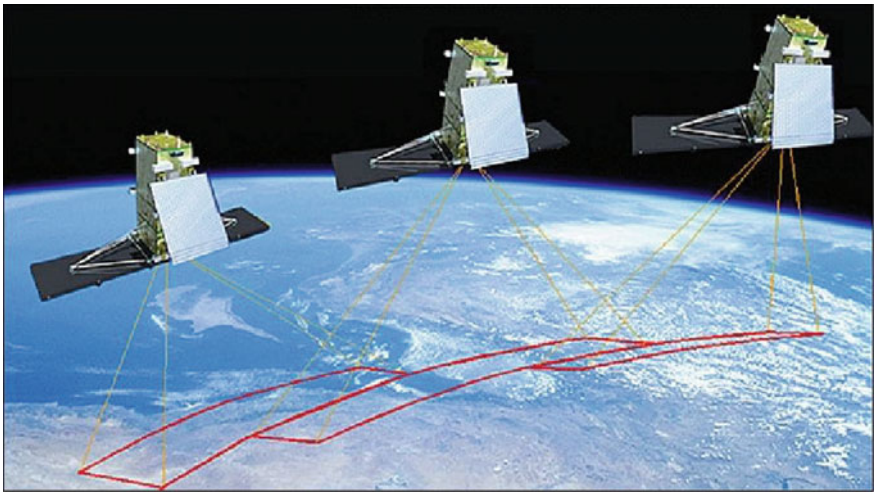

Fig. 2.37 Artist's rendition of the RCM imaging concept (image credit: MDA, CSA) (https://directory.eoportal.org/web/eoportal/satellite-missions/r/rcm)

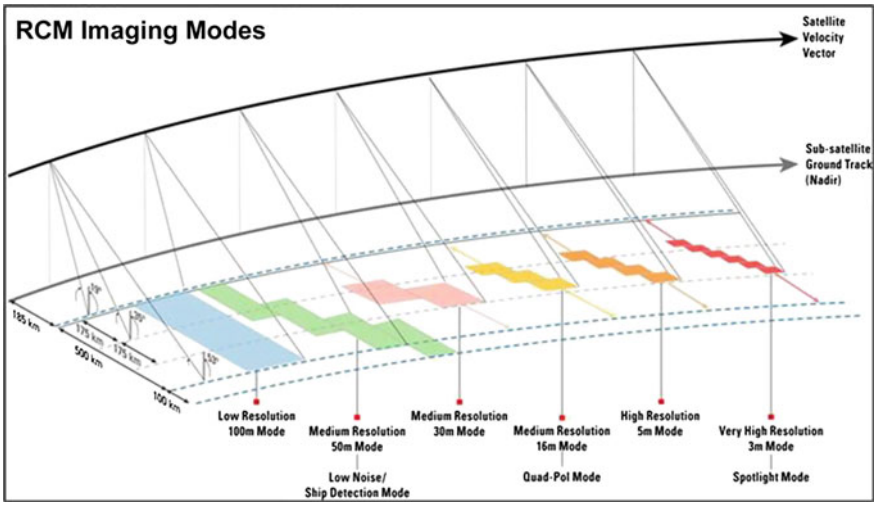

Fig. 2.38 Imaging modes of Radar Constellation Mission (RCM) (Credit: Canadian Space Agency)

and atmosphere) using a variety of measurement principles. A tenth instrument, DORIS, provided guidance and control. Several of the instruments are advanced versions of instruments that were flown on the earlier ERS 1 and ERS 2 missions and other satellites.

Advanced Synthetic Aperture Radar (ASAR)

ASAR (Advanced Synthetic Aperture Radar) operates in the C-band in a wide variety of modes. It can detect changes in surface heights with sub millimetre precision. It served as a data link for ERS 1 and ERS 2, providing numerous functions such as observations of different polarization of light or combining different polarization, angles of incidence and spatial resolutions. The characteristics of ASAR instrument is shown in Table 2.13.

Other instruments aboard Envisat include AATSR (Advanced Along-Track Scanning Radiometer), MERIS (Medium Resolution Imaging Spectrometer), SCIAMACHY (Scanning Imaging Absorption spectrometer for Atmospheric CHartographY), RA-2 (RadarAltimeter 2), MWR (Microwave Radiometer), DORIS (Doppler Orbitography and Radiopositioning Integrated by Satellite), GOMOS (Global Ozone Monitoring by Occultation of Stars), MIPAS (Michelson Interferometer for Passive Atmospheric Sounding) and, ESA formally announced the end of Envisat's mission on 9 May 2012. The mission has been replaced by the Sentinel series of satellites. The first of these—Sentinel 1A—was launched on 13 April 2014.

2.7.8 Radar Imaging Satellite (RISAT) Missions

So far, two missions have been launched. A brief detail of missions is presented hereafter.

Table 2.13 Salient features of different beam modes of Radarsat-2 mission

Beam modes	Nominal swath width (km)	Approximate resolution (m)
Selective polarization transmit H or V, receive H and/or V		
Fine	50	10 × 9
Standard	100	25 × 28
Low incidence	170	40 × 28
High incidence	75	20 × 28
Wide	150	25 × 28
ScanSAR narrow	300	50 × 50
ScanSAR wide	500	100 × 100
Polarimetric transmit H and V on alternate pulses/receive H and V on any pulse		
Fine Quad-pol	25	11 × 9
Standard Quad-pol	25	25 × 28
Selective single polarization transmit H or V, receive H or V		
Ultra-Fine	20	3 × 3
Spotlight	18	3 × 1
Multi-Look fine	50	11 × 9

2.7.8.1 Radar Imaging Satellite (RISAT-2)

Radar Imaging Satellite-2 (RISAT-2) was launched on 20 April 2009 by the Indian Space research organization. RISAT-2 with the Synthetic Aperture Radar (SAR) sensor can provide images with 1 m resolution. It has a revisit period of 3 or 4 days and a repeat cycle of 14 days. The highly agile bus design, in combination with the body-pointing parabolic dish antenna system, permits increased viewing capabilities from the spacecraft. The spacecraft/antenna system may be dynamically redirected to any direction of the flight path (i.e. in the cross-track as well as in the along-track direction). Thus, a wide FOR (Field of Regard) within the incidence angle range may be obtained on either side of the ground track for event monitoring coverage. The multimode SAR is capable of high-resolution imaging in Spot (1 m), Strip (3 m), Mosaic (1.8 m) and wide coverage (8 m) modes as in Table 2.14.

Strip Mode

The synthetic apertures are targeted on wide geographical swaths. The spacecraft performs synchronous imaging and does not change its orientation during observations except for some small manoeuver to keep the imaging strip parallel to the ground track. Squinted strip imaging is also possible.

Wide Coverage ScanSAR

The coverage of large strips is achieved by electronic beam steering. Three beams are used in the nominal wide coverage mode, which create three footprints (sub-swaths) in the target area. The ground resolution in this mode decreases since the integration time is split up among the sub-swaths. The swath width can be increased, by using more antenna beams. In principle, the swath width may get to more than 100 km for some incidence angles. However, this reduces the ground resolution to about 20 m.

Spotlight Mode

This focuses on specific, pre-assigned target. In spotlight, the spacecraft performs mechanical steering to halt the antenna footprint in a specific target area. The longer integration time over the spot target area yields an improved azimuth resolution. The range resolution is achieved by adjusting the bandwidth to the incidence angle.

Table 2.14 Characteristics of ASAR sensor

Mode	Polarization	Incidence	Resolution	Swath
Alternating polarization	HH/VV, HH/HV, VV/VH	15–45°	30–150 m	58–110 km
Image	HH, VV	15–45°	30–150 m	58–110 km
Wave	HH, VV		400 m	5 × 5 km
Suivi global (ScanSAR)	HH, VV		1 km	405 km
Wavescan (ScanSAR)	HH, VV		150 m	405 km

The ability for spotlight imaging in squint allows for multi-look imaging without any loss in resolution. To obtain a multi-look image of a given target area, a number of spotlight images are observed, each at a different squint angle.

Mosaic Mode

The radar imager slews its focus on a number of spots in the same general target area. The mosaic mode enables to extend the limited coverage of the spot mode by using the electronic steering capability of XSAR. In mosaic mode, the radar beam scans in the range direction while the mechanical manoeuvering advances the strip line in the azimuth direction. Hence, this mode may also be interpreted as the spot version of ScanSAR.

2.7.8.2 Radar Imaging Satellite (RISAT-1)

The Radar Imaging Satellite (RISAT-1), launched by Indian Space Research Organization (ISRO) on 26 April 2012 was successfully placed in the polar Sun-synchronous orbit of 536 km height. RISAT-1 carries a multimode C-band (5.35 GHz) Synthetic Aperture Radar (SAR) as the payload with the capability of imaging in HH, VV, HV, VH and circular polarizations. As it is a side-looking active sensor, around 107 km of either side of the sub-satellite track comes under non-imageable area for the orbit under consideration.

Imaging Geometry and Modes of Operation

RISAT-1 is operated in the following modes in different polarizations (Table 2.15). In the absence of the emergency/user request, the default mode of collection will be MRS descending, left looking, with dual polarization with a repeat cycle of 25 days (Fig. 2.39).

2.7.9 Soil Moisture and Ocean Salinity Mission (SMOS)

Known as 'Water Mission', the Soil Moisture and Ocean Salinity (SMOS) mission was launched on 2 November 2009 (Fig. 2.40). The mission with Sun-synchronous

Table 2.15 Imaging modes of RISAT-2 SAR

VHD mode number	Radar mode	Resolution (m)
1	Spot A	1
2	Spot B	1 × 2
4	Strip	3
5	Super Strip	1.8
6	Wide C	8
8	Mosaic1	1
10	Mosaic3	3

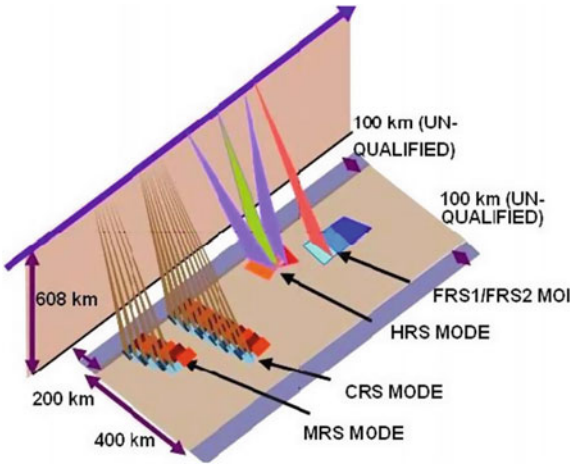

Fig. 2.39 RISAT-1 SAR imaging modes

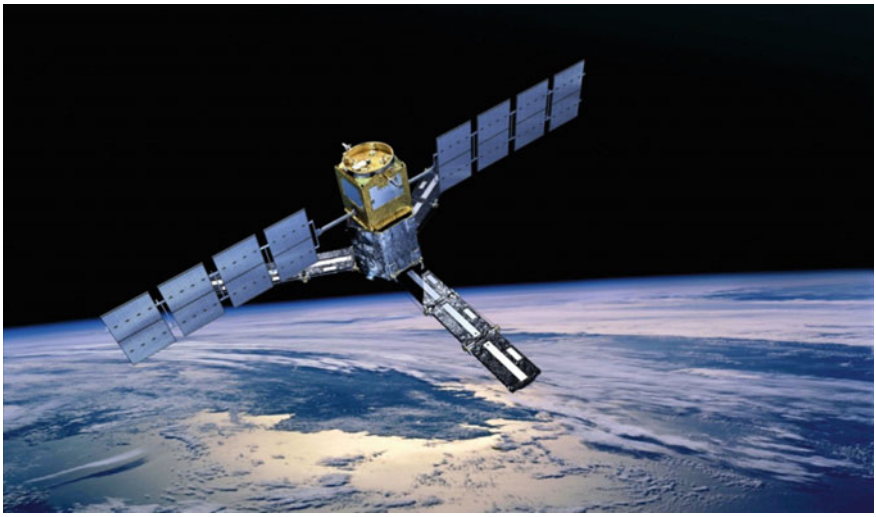

Fig. 2.40 SMOS mission: An artist's view (SMOS http://www.esa.int/Our_Activities/Observing_the_Earth/SMOS/Instrument)

polar orbit and orbital period of 100 ± 15 min and local equator crossing time at 6:00 AM on ascending node has a repeat cycle of 23 days and a 3-day sub-cycle. The main objective of SMOS mission is to demonstrate observations of sea surface salinity (SSS) over oceans and soil moisture over land to advance climatologic, meteorologic, hydrologic and oceanographic applications. The mission also aims at providing observations over snow- and ice-covered regions, contributing to the study of the cryosphere. The satellite carries a L-band (1.4 GHz.) radiometer known

as Microwave Imaging Radiometer with Aperture Synthesis (MIRAS), which provides the best sensitivity to variations of moisture in the soil and changes in the salinity of the ocean, coupled with minimal disturbance from weather, atmosphere and vegetation cover. In order to achieve the spatial resolution required for observing soil moisture and ocean salinity, the laws of physics mean that to take measurements in L-band, a huge antenna would have been required—too big for a satellite to carry. To overcome this challenge, the antenna needed for MIAS has been simulated through 69 small antennas, distributed over the three arms and central hub of the instrument.

During the launch, the three deployable arms are folded up, but once SMOS is in orbit each of the arms folds out into an unusual three-pointed star shape. Hence, with a diameter of eight meters, MIRAS is often dubbed a 'star in the sky'. The 69 antenna elements, called LICEFs, are antenna-receiver integrated units, each measure radiation emitted from Earth's surface at L-band. One LICEF antenna, weighs 190 g, is 165 mm in diameter and 19 mm high.

The mission with Sun-synchronous polar orbit and orbital period of 100 ± 15 min and local equator crossing time at 6:00 AM on ascending node has a repeat cycle of 23 days and a 3-day sub-cycle.

2.7.9.1 Measurement Principle

For optimum results, SMOS measures microwave radiation emitted from Earth's surface within the L-band (1.4 GHz) using an interferometric radiometer. The SMOS radiometer exploits the interferometry principle, which by way of 69 small receivers measures the phase difference of incident radiation. The mission approach is in Table 2.16. The technique is based on cross-correlation of observations from all possible combinations of receiver pairs. A two-dimensional 'measurement image' is taken every 1.2 s. As the satellite moves along its orbital path each observed area is seen under various viewing angles. From an altitude of

Table 2.16 Salient features of SMOS mission

Instrument	Microwave imaging radiometer using aperture synthesis—MIRAS
Frequency	L-band (21 cm–1.4 GHz)
Number of receivers	69
Receiver spacing	0.875 lambda = 18.37 cm
Polarisation	H & V (polarimetric mode optional)
Spatial resolution	35 km at centre of field of view
Tilt angle	32.5°
Radiometric resolution	0.8–2.2 K
Angular range	0–55°
Temporal resolution	3-days revisit at Equator
Instrument data rate	89 kbps H & V pol.

Source Kerr et al. (2001)

around 758 km, the antenna views an area of almost 3000 km in diameter. However, due to the interferometry principle and the Y-shaped antenna, the field of view is limited to a hexagon-like shape about 1000 km across called the 'alias-free zone'. This area corresponds to observations where there is no ambiguity in the phase difference. The MIRAS instrument has three main operational modes: (i) Dual-polarization mode, in which all receivers are switched synchronously to either H or V polarization; (ii) Full polarimetric mode, in which segments of the array are switched according to a predefined sequence between H and V; and (iii) Calibration modes, in which measurements of the internal load, the noise diodes or the so-called "fringe washing function" are determined.

2.7.10 Soil Moisture Active Passive Mission (SMAP)

Launched on 13 January 2015 into a 680 km near-polar, Sun-synchronous orbit, with equator crossings at 6 am and 6 pm local time SMAP provides global measurements of soil moisture and its freeze/thaw state (Fig. 2.41). These measurements are intended to be used to enhance understanding of processes that link the water, energy and carbon cycles, and to extend the capabilities of weather and climate prediction models. SMAP data will also be used to quantify net carbon flux

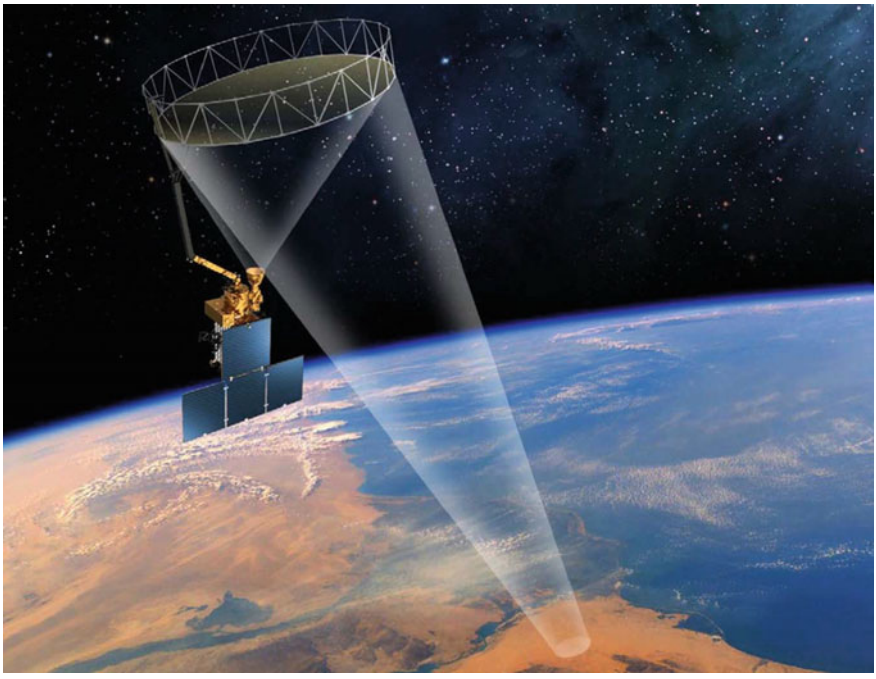

Fig. 2.41 SMAP mission: an artist's view (http://smap.jpl.nasa.gov/data/)

Table 2.17 Salient features of SMAP-SAR and radiometer

	SAR	Radiometer
Frequency	1.2 GHz	1.41 GHz
Polarizations	VV, HH, HV	V, H, U
Resolution	1.3 km[a]	40 km
Antenna Diameter	6 m	
Rotation rate	14.6 rpm	
Incidence angle	40°	
Swath width	1000 km	
Orbit	Polar, Sun-synchronous	
Local time ascending node	6 am	
Altitude	670 km	

[a]Over outer 70% of swath

in boreal landscapes and to develop improved flood prediction and drought monitoring capabilities. The salient features of SMAP System characteristics are shown in Table 2.17.

The SMAP instrument includes a radiometer and synthetic aperture radar operating at L-band (1.20–1.41 GHz). The instrument is designed to make coincident measurements of surface emission and backscatter, with the ability to sense the soil conditions through moderate vegetation cover. The measurement swath width is 1000 km, providing global coverage within 3 days at the equator and 2 days at boreal latitudes (>45° N). On 7 July 2015 SMAP-SAR stopped transmitting data, and on 2 September 2015 NASA announced the amplifier failure. The sensor is now no more functional.

2.8 Conlusions

In a quest to furthering our understanding about the Earth and its environment the field spectroscopy was first used in the late fifties (Penndorf 1956). With the subsequent scientific and technological advancements, the developments in sensors not only in terms of the regions of the electromagnetic spectrum covered but also with respect to spatial, spectral, radiometric resolutions have taken place. Such developments have catered to the requirements of the management of natural resources and environment and infrastructure developments. More importantly, the improved temporal resolution and global coverage, the ability of the sensors to measure the atmospheric and oceanic phenomena has provided a very good handle to study the various facets of hydrological and bio-geochemical cycles leading ultimately to providing an insight into the phenomenon of the global climatic change. Though an attempt has been made to provide an overview of the Earth-observing mission, owing to a very large number of such missions, only a few important ones have been covered. Nevertheless, it is hoped that such information will enable the readers

to get insight into various aspects sensors and platforms and the modes of data acquisition that may facilitate selection of the appropriate data for various applications

References

Cracknell, A.P. and Hayes, 2007, Introduction to Remote Sensing. CRC Press, Taylor & Francis Group.

Curran, P.J. 1988. Principles of remote sensing. …… Chugh Publications.

Eastman, F.H. 1970. A high-resolution image sensor. Journal of the Society of Motion Picture and Television Engineers 79, 10–15.

Elachi, C. 1987. Spaceborne Radar Remote Sensing: Applications and Techniques. IEEE Press, New York.

Hamlyn, G.J. and Vaughan, R.A. 2010, Remote Sensing of Vegetation: Principles, Techniques, and Applications. OUP Oxford.

Hug, C., Ullrich, A., Grimm, A., 2004. Litemapper-5600—A waveform-digitizing LIDAR terrain and vegetation mapping system. International Archives of Photogrammetry, Remote Sensing and Spatial Information Sciences, 36 (Part 8/W2) (2004), pp. 24–29.

Joseph, G., 2003. Fundamentals of Remote Sensing. Hyderabad: University Press, 433 pp.

Kerr, Y.H., P Waldteufel, JP Wigneron, J Martinuzzi, J Font, M Berger, 2001. Soil moisture retrieval from space: the Soil Moisture and Ocean Salinity (SMOS) mission IEEE transactions on Geosciences and remote sensing 39(8), 1729–1735.

Pendorf, R., 1956. Luminous and spectral reflectance as well colour of natural objects. U.S. Air Force Research Centre, Bedford. Massachusetts.

Rees, Gareth. (1999), The Remote Sensing Data Book. Cambridge University Press.

Schultz, G.A., and Engman, 2000. E.T.Remote sensing in hydrology and water resources management. Springer.

Toutin, Thierry; Beaudoin, Marc (1995) "Real-time extraction of planimetric and altimetric features from digital stereo SPOT data using a digital video plotter," Photogrammetric Engineering and Remote Sensing: vol. 61(1); pp 63–68.

Ulaby, F.T.; Dobson, M.C.; Bradley, G.A. Radar reflectivity of bare and vegetation-covered soil. Adv. Space Res. 1981, 1, 91–104.

Ulaby, F.T., Moore, R.K. and Fung, A.K., 1982. Microwave Remote Sensing, Vol. 2: Radar Remote Sensing and Surface Scattering and Emission Theory. Addison-Wesley, Reading M.A.

URLS

Airborne Laser Scanning (U. Idaho). http://classes.css.wsu.edu/soils374/ppt/lidar2.pdf.

LiDAR in forestry workshop. http://www.softree.com/articles/LiDARWorkshop.pdf.

Landsat System. https://directory.eoportal.org/web/eoportal/satellite-missions/l/landsat-1-3.

Source: LiDAR technology overview. http://carms.geog.uvic.ca/LiDAR%20Web%20Docs/LiDAR%20paper%20june%202006.pdf.

Source: http://www.google.co.in/url?sa=t&rct=j&q=&esrc=s&source=web&cd=12&sqi=2&ved=0CF4QFjAL&url=http%3A%2F%2Fwww.grss-ieee.org%2Fwp-content%2Fuploads%2F2010%2F06%2FRadar_Interferometry_Part1.pdf&ei=Das_VKnuKdCMuATfwYLQDA&usg=AFQjCNHeglizewi5KFlSYppplJxXDiaOnw&sig2=OuNsoc0XTyYHoVp3MURbBA.

http://blackbridge.com/rapideye/news/pr/2013-blackbridge.htm.

https://directory.eoportal.org/web/eoportal/satellite-missions/content/-/article/smos.
http://space.skyrocket.de/doc_sdat/rapideye-1.htm.
http://en.wikipedia.org/wiki/China%E2%80%93Brazil_Earth_Resources_Satellite_program.
http://en.wikipedia.org/wiki/Interferometric_synthetic_aperture_radar.
http://en.wikipedia.org/wiki/Landsat_program.
http://en.wikipedia.org/wiki/Satellite_constellation.
http://en.wikipedia.org/wiki/Sentinel-1.
http://eo1.usgs.gov.
http://eo1.usgs.gov/sensors/ali.
http://eo1.usgs.gov/sensors/leisa.
http://imaging.geocomm.com/features/sensor/radarsat1/.
http://landsat.gsfc.nasa.gov/about/ldcm.html.
http://noaasis.noaa.gov/NOAASIS/ml/avhrr.html.
http://nsidc.org/data/docs/daac/amsre_instrument.gd.html.
http://uregina.ca/piwowarj/Satellites/IRS.html.
http://www.angelfire.com/co/pallav/sensorindian.html.
http://www.asc-csa.gc.ca/eng/satellites/radarsat/radarsat-tableau.asp.
http://www.asc-csa.gc.ca/eng/satellites/smos/.
http://www.astrium-geo.com/en/147-spot-6-7-satellite-imagery.
http://www.crisp.nus.edu.sg/∼research/tutorial/spot.htm.
http://www.esa.int/Our_Activities/Observing_the_Earth/SMOS/Instrument.
http://www.google.co.in/url?sa=t&rct=j&q=&esrc=s&source=web&cd=18&ved=0CEAQFjAHOAo&url=http%3A%2F%2Fwww.oregonstatehospital.net%2Fd%2Fotherfiles%2FInterferometry.pdf&ei=OAxjVLmUO8q9ugSDpIGwCw&usg=AFQjCNHyGAt8QE4dh6V3q0agd-qoGYYekQ&bvm=bv.79189006,d.c2E).
http://www.isro.org/satellites/cartosat-2b.aspx.
http://www.nasaspaceflight.com/2014/06/indias-pslv-successfully-lofts-spot-7-companions/.
http://www.satimagingcorp.com/satellite-sensors/other-satellite-sensors/rapideye/.
http://www.satimagingcorp.com/satellite-sensors/pleiades-1/.
http://www.satimagingcorp.com/satellite-sensors/worldview-2/.
http://www.satimagingcorp.com/satellite-sensors/worldview-3/.
http://www2.hawaii.edu/∼jmaurer/terra/.
http://www2.hawaii.edu/∼jmaurer/terra/.
https://www.google.co.in/?gws_rd=ssl#q=spot-4+satellite+High+Resolution+Vertical+Infrared+%28HRV-IR.
https://www-misr.jpl.nasa.gov/Mission/.
www.jars1974.net/pdf/03_Chapter02.pdf.

http://www.springer.com/978-3-662-53738-1

Remote Sensing of Soils
Ravi Shankar, D.
2017, XXVII, 500 p. 166 illus., Hardcover
ISBN: 978-3-662-53738-1